

Cooperative Diastereoselectivity of Palladium- and Platinum-Promoted Intramolecular [4+2] Diels–Alder Cycloaddition Reactions of 3,4-Dimethyl-1-phenylphosphole

Kent D. Redwine, William L. Wilson, Donald G. Moses, Vincent J. Catalano, and John H. Nelson*

Department of Chemistry/216, University of Nevada—Reno, Reno, Nevada 89557-0020

Received July 26, 1999

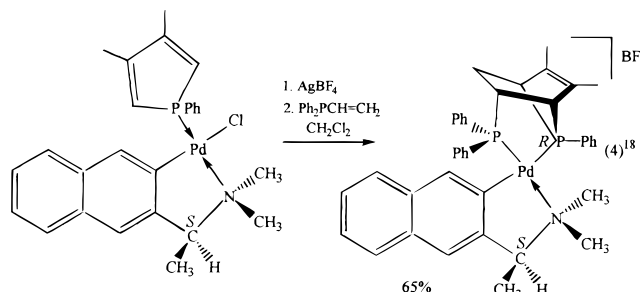
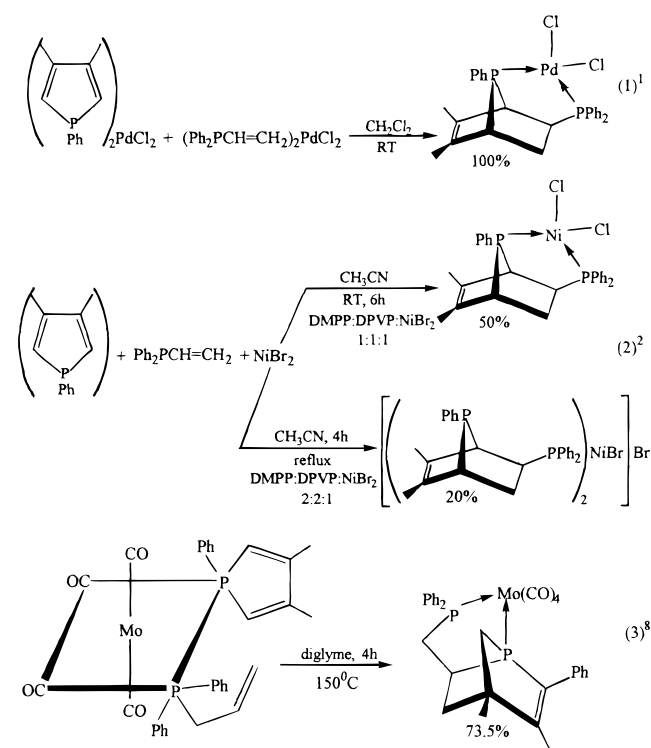
The complexes $[(\text{DMPP})_2\text{M}(\text{CH}_3\text{CN})_2]\text{X}_2$ (DMPP = 3,4-dimethyl-1-phenylphosphole; M = Pd, Pt; X = BF_4^- , NO_3^- , ClO_4^-) react with 2 equiv of the dienophiles *N,N*-dimethylacrylamide (DMAA), 2-vinylpyridine (VyPy), and diphenylvinylphosphine (DPVP) to form bis-[4+2] Diels–Alder cycloaddition products. The $[\text{M}(\text{DMPP})_2(\text{DMAA})_2]^{2+}$ and $[\text{M}(\text{DMPP})_2(\text{VyPy})_2]^{2+}$ complexes form exclusively as the *cis*-geometric isomers, whereas for $[\text{M}(\text{DMPP})_2(\text{DPVP})_2]^{2+}$, both *cis*- and *trans*-geometric isomers are formed. The two Diels–Alder cycloadditions occur sequentially, and the absolute configuration of the first reaction influences the absolute configuration of the second. In all cases, racemic mixtures of the (*R,R*) and (*S,S*) diastereomers are formed; none of the meso (*R,S*) diastereomer is observed. New complexes were characterized by elemental analyses, physical properties, infrared spectroscopy, ^1H , $^1\text{H}\{^{31}\text{P}\}$, $^{13}\text{C}\{^1\text{H}\}$, and $^{31}\text{P}\{^1\text{H}\}$ NMR spectroscopy, and, in most cases, X-ray crystallography.

Introduction

We have employed the highly efficient, diastereoselective transition metal promoted intramolecular [4+2] Diels–Alder cycloaddition reactions of 1*H*-phospholes^{1–7} and 2*H*-phospholes⁸ with a variety of dienophilic ligands to form a number of conformationally rigid asymmetric chelating ligands. The scope and diastereoselectivity of these reactions depend on the nature of the metal and its ancillary ligands as illustrated in reactions 1–3.

Reactions 1–3 only occur with vinyl- or allylphosphines as dienophiles, and in each case, racemic products are formed.

Recently, organopalladium complexes containing optically pure forms of orthopalladated [1-(dimethylamino)ethyl]naphthalene^{9–17} and [2-(dimethylamino)ethyl]naphthalene¹⁸ were used as chiral templates to promote asymmetric modifications of several of these reactions. An example is shown in reaction 4.



(1) Rahn, J. A.; Holt, M. S.; Gray, G. A.; Alcock, N. W.; Nelson, J. H. *Inorg. Chem.* **1989**, 28, 217.

- (2) Solujić, Lj.; Milosavljević, E. B.; Nelson, J. H.; Alcock, N. W.; Fischer, J. *Inorg. Chem.* **1989**, 28, 3453.
 (3) Affandi, S.; Nelson, J. H.; Fischer, J. *Inorg. Chem.* **1989**, 28, 4536.
 (4) Bhaduri, D.; Nelson, J. H.; Day, C. L.; Jacobson, R. A.; Solujić, Lj.; Milosavljević, E. B. *Organometallics* **1992**, 11, 4069.
 (5) Ji, H.-L.; Nelson, J. H.; DeCian, A.; Fischer, J.; Solujić, Lj.; Milosavljević, E. B. *Organometallics* **1992**, 11, 1840.
 (6) Nelson, J. H. In *Phosphorus-31 NMR Spectral Properties in Compound Characterization and Structural Analysis*; Quin, L. D., Verkade, J. G., Eds.; VCH: Deerfield Beach, FL, 1994; pp 203–214.
 (7) Redwine, K. D.; Catalano, V. J.; Nelson, J. H. *Synth. React. Inorg. Met.-Org. Chem.* **1999**, 29, 395.
 (8) Maitra, K.; Catalano, V. J.; Nelson, J. H. *J. Am. Chem. Soc.* **1997**, 119, 12560.
 (9) Leung, P.-H.; Loh, S. H.; Mok, K. F.; White, A. J. P.; Williams, D. J. *J. Chem. Soc., Chem. Commun.* **1996**, 591.
 (10) Aw, B. H.; Leung, P.-H.; White, A. J. P.; Williams, D. J. *Organometallics* **1996**, 15, 3640.
 (11) Selvaratnam, S.; Mok, K. F.; Leung, P.-H.; White, A. J. P.; Williams, D. J. *Inorg. Chem.* **1996**, 35, 4798.
 (12) Leung, P.-H.; Loh, S. K.; Mok, K. F.; White, A. J. P.; Williams, D. J. *J. Chem. Soc., Dalton Trans.* **1996**, 4443.

Table 1. ^1H and $^{31}\text{P}\{^1\text{H}\}$ NMR Data for $[(\text{DMPP})_2\text{M}(\text{NO}_3)_2]$ (**1a,b**)

M	solvent	temp ($^\circ\text{C}$)	$\delta(^{31}\text{P})$ ($^1\text{J}(\text{PtP})$)	$\delta(^1\text{H})$			
				Ph	H_α ($ ^2\text{J}(\text{PH}) + ^4\text{J}(\text{PH}) $)	CH_3CN	CH_3
Pd	CD_3NO_2	25	37.6	7.20–7.45 (m)	6.41 (34.5 Hz)		2.07
Pd	CD_3CN	25	39.3	7.42–7.66 (m)	6.42 (35.5 Hz)	2.01	2.16
Pt	CD_3NO_2	25	7.96 (3663 Hz)	7.40–7.70 (m)	6.34 (33.5 Hz)		2.08
Pt	CD_3CN	25	{17.02 (3159 Hz) ^a 11.63 (3472 Hz) ^a }	7.38–7.70 (m)	6.35 (33.5 Hz)	2.03	2.12
Pt	CD_3CN	75	{10.42 (3667 Hz) ^b 9.93 (3652 Hz) ^b }				

^a *cis*- $[(\text{DMPP})_2\text{Pt}(\text{CD}_3\text{CN})(\text{NO}_3)]^+$. ^b *cis*- $[(\text{DMPP})_2\text{Pt}(\text{CD}_3\text{CN})_2]^{2+}$.

Disolvento bis(phosphine) complexes of palladium(II)¹⁹ and platinum(II)²⁰ of the type $[(\text{R}_3\text{P})_2\text{M}(\text{S})_2]^{2+}$ (S = solvent) are readily prepared by reactions of $[(\text{R}_3\text{P})_2\text{MCl}_2]$ complexes with a silver salt of a weakly coordinating anion in a donor solvent. We reasoned that similar reactions of $[(\text{DMPP})_2\text{PdCl}_2]$ ^{21,22} and $[(\text{DMPP})_2\text{PtCl}_2]$ ^{23,24} (DMPP = 3,4-dimethyl-1-phenylphosphole) with AgBF_4 , AgNO_3 , or AgClO_4 in CH_3CN followed by addition of 2 equiv of a dienophilic ligand such as *N,N*-dimethylacrylamide (DMAA), 2-vinylpyridine (VyPy), or diphenylvinylphosphine (DPVP) might lead to two sequential metal-promoted intramolecular [4+2] Diels–Alder cycloadditions. Complementarity²⁵ in the fitting of the two conformationally rigid chiral asymmetric bidentate ligands around the metal center could then provide for asymmetric induction and the preferential formation of homochiral (*R,R*) and (*S,S*) diastereomers rather than the formation of the internally compensated meso (*R,S*) diastereomers. The diastereoselectivities of these reactions are described herein.

Results and Discussion

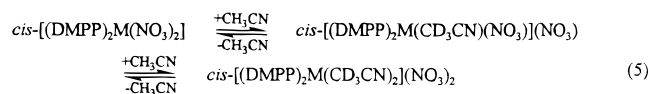
Synthesis and Characterization of $[(\text{DMPP})_2\text{M}(\text{NO}_3)_2]$. The chloro complexes $[(\text{DMPP})_2\text{MCl}_2]$ (M = Pd,^{21,22} Pt^{23,24}) react cleanly with 2 equiv of AgNO_3 in CH_3CN solution at ambient temperature to form AgCl and pale yellow and colorless crystals of *cis*- $[(\text{DMPP})_2\text{Pd}(\text{NO}_3)_2]$ (**1a**) and *cis*- $[(\text{DMPP})_2\text{Pt}(\text{NO}_3)_2]$ (**1b**), respectively. Infrared spectra of their Nujol mulls exhibit ν_{NO} vibrations at 1480, 1440, 1282, 1262, 1004, and 786 cm^{-1} (**1a**) and 1493, 1456, 1281, 1261, 989, and 789 cm^{-1} (**1b**), similar to the data reported²⁶ for $[(\text{Ph}_3\text{P})_2\text{Pt}(\text{NO}_3)_2]$. In CD_3CN solutions, these complexes are in equilibrium with the solvento species *cis*- $[(\text{DMPP})_2\text{Pd}(\text{CD}_3\text{CN})_2]^{2+}$, *cis*- $[(\text{DMPP})_2\text{Pt}(\text{CD}_3\text{CN})(\text{NO}_3)]^+$, and *cis*- $[(\text{DMPP})_2\text{Pt}(\text{CD}_3\text{CN})_2]^{2+}$ (reaction

Table 2. Crystallographic Data for $[(\text{DMPP})_2\text{Pd}(\text{NO}_3)_2]$ (**1a**) and $[(\text{DMPP})_2\text{Pt}(\text{NO}_3)_2]$ (**1b**)

	1a	1b
empirical formula	$\text{C}_{24}\text{H}_{26}\text{N}_2\text{O}_6\text{P}_2\text{Pd}$	$\text{C}_{24}\text{H}_{26}\text{N}_2\text{O}_6\text{P}_2\text{Pt}$
fw	606.81	695.50
crystal system	orthorhombic	orthorhombic
space group	<i>Pbca</i>	<i>Pbca</i>
Z	8	8
<i>a</i> (\AA)	18.462(2)	18.537(2)
<i>b</i> (\AA)	13.719(2)	13.7270(9)
<i>c</i> (\AA)	20.356(2)	20.392(2)
<i>V</i> (\AA^3)	5156.0(9)	5189.0(9)
ρ_{calc} (g cm^{-3})	1.563	1.781
<i>T</i> ($^\circ\text{C}$)	25	25
μ (cm^{-1})	8.85	55.73
$\text{R1}(F)^a$ [$I > 2\sigma(I)$]	0.0394	0.0529
$\text{wR2}(F^2)^b$	0.0968	0.0857
GOF	1.021	1.001

^a $\text{R1}(F) = \sum ||F_o| - |F_c|| / \sum |F_o|$. ^b $\text{wR2}(F^2) = \{\sum [w(F_o^2 - F_c^2)^2] / \sum [w(F_o^2)^2]\}^{0.5}$.

5), as evidenced by the ^1H and $^{31}\text{P}\{^1\text{H}\}$ NMR spectra recorded in CD_3NO_2 and CD_3CN (Table 1). The populations of the



solvento species increase with increasing temperature, suggesting that nitrate is a better donor to palladium(II) and platinum(II) than CD_3CN .

Crystallization from an CH_3CN /ether mixture provided X-ray-quality crystals. Crystallographic data are listed in Table 2. Views of the structures of **1a** and **1b** are shown in Figures 1 and 2. These two compounds are isomorphous and isostructural. They both possess *cis* geometries. Even though they contain coordinated CH_3CN in CH_3CN solutions, from which the crystals were isolated, they do not contain coordinated CH_3CN in the solid state, consistent with equilibrium 5 lying to the left. They are rigorously planar, as the sums of the angles around the metals are $360.1(1)^\circ$ in both cases. They contain monodentate nitrate ions, as suggested by infrared spectroscopy.²⁷ The M–P distances are essentially the same (2.2455 \AA , average, Pd; 2.226 \AA , average, Pt) as are the M–O distances (2.111 \AA , average, Pd; 2.092 \AA , average, Pt). The latter are comparable to the Pd–O distances (2.066 \AA) reported²⁸ for *cis*- $[(\text{Me}_2\text{SO})_2\text{Pd}(\text{NO}_3)_2]$. The Pd–P distances are similar to those in *cis*- $[(\text{DMPP})_2\text{PdCl}_2]$ (2.291 \AA , average).²¹

Reactions of $[(\text{DMPP})_2\text{M}(\text{CH}_3\text{CN})_2]\text{X}_2$ with the Dienophilic Ligands DMAA, VyPy, and DPVP. After addition of 2 equiv of AgX (X = BF_4^- , NO_3^- , ClO_4^-) to a solution of 1

- (13) Aw, B. H.; Hor, T. S. A.; Selvaratnam, S.; White, A. J. P.; Williams, D. J.; Rees, N. H.; McFarlane, W.; Leung, P.-H. *Inorg. Chem.* **1997**, *36*, 2138.
- (14) Leung, P.-H.; Selvaratnam, S.; Cheng, C. R.; Mok, K. F.; Rees, N. H.; McFarlane, W. *J. Chem. Soc., Chem. Commun.* **1997**, 751.
- (15) Liu, A. M.; Mok, K. F.; Leung, P.-H. *J. Chem. Soc., Chem. Commun.* **1997**, 2397.
- (16) Leung, P.-H.; Siah, S. Y.; White, A. J. P.; Williams, D. J. *J. Chem. Soc., Dalton Trans.* **1998**, 893.
- (17) Song, Y.; Vittal, J. J.; Chan, S.-H.; Leung, P.-H. *Organometallics* **1999**, *18*, 650.
- (18) Gül, N.; Nelson, J. H. *Tetrahedron* **2000**, *56*, 71.
- (19) Hartley, F. R.; Murray, S. G.; Wilkinson, A. *Inorg. Chem.* **1989**, *28*, 549 and references therein.
- (20) Siegmund, K.; Pregosin, P. S.; Venanzi, L. M. *Organometallics* **1989**, *8*, 2659.
- (21) MacDougall, J. J.; Cary, L. W.; Mayerle, J.; Mathey, F.; Nelson, J. H. *Inorg. Chem.* **1980**, *19*, 709.
- (22) Wilson, W. L.; Fischer, J.; Wasylshen, R. E.; Eichele, K.; Catalano, V. J.; Frederick, J. H.; Nelson, J. H. *Inorg. Chem.* **1996**, *35*, 1486.
- (23) MacDougall, J. J.; Nelson, J. H.; Mathey, F. *Inorg. Chem.* **1982**, *21*, 2145.
- (24) Wilson, W. L.; Rahn, J. A.; Alcock, N. W.; Fischer, J.; Frederick, J. H.; Nelson, J. H. *Inorg. Chem.* **1994**, *33*, 109.
- (25) Bray, K. L.; Butts, C. P.; Lloyd-Jones, G. C.; Murray, M. *J. Chem. Soc., Dalton Trans.* **1998**, 1421.
- (26) Cook, C. D.; Jauhal, G. S. *J. Am. Chem. Soc.* **1967**, *89*, 3066.

- (27) Nakamoto, K. *Infrared and Raman Spectra of Inorganic and Coordination compounds*, 5th ed.; Wiley-Interscience: New York, 1997; Parts A and B.
- (28) Langs, D. A.; Hare, C. R.; Little, R. G. *J. Chem. Soc., Chem. Commun.* **1967**, 1080.

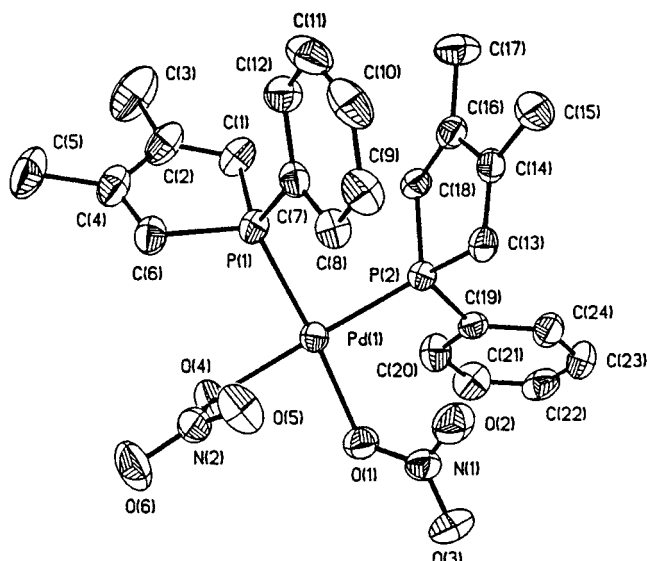


Figure 1. Structural drawing of $[(\text{DMPP})_2\text{Pd}(\text{NO}_3)_2]$ (**1a**), showing the atom-numbering scheme (40% probability ellipsoids). Selected bond distances (Å) and bond angles (deg): Pd(1)–O(1), 2.101(3); Pd(1)–O(4), 2.121(3); Pd(1)–P(1), 2.2436(12); Pd(1)–P(2), 2.2473(11); O(1)–Pd(1)–O(4), 84.13(12); P(1)–Pd(1)–P(2), 91.78(4); O(1)–Pd(1)–P(2), 93.20(9); O(4)–Pd(1)–P(1), 90.99(9).

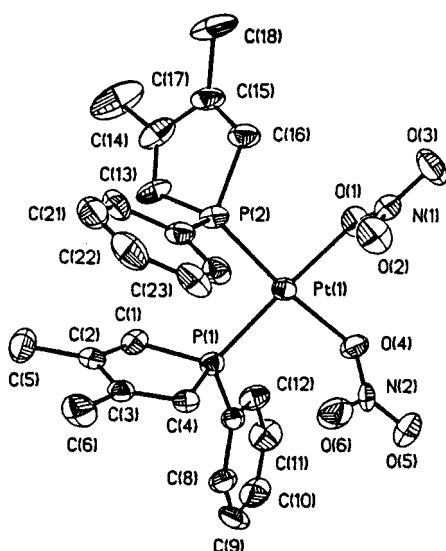
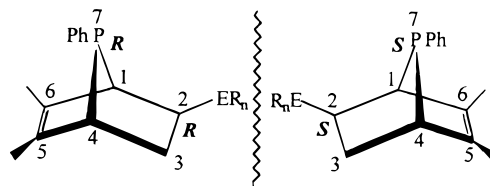


Figure 2. Structural drawing of $[(\text{DMPP})_2\text{Pt}(\text{NO}_3)_2]$ (**1b**), showing the atom-numbering scheme (40% probability ellipsoids). Selected bond distances (Å) and bond angles (deg): Pt(1)–O(1), 2.098(8); Pt(1)–O(4), 2.085(7); Pt(1)–P(1), 2.227(3); Pt(1)–P(2), 2.225(3); O(1)–Pt(1)–O(4), 82.8(3); P(1)–Pt(1)–P(2), 93.50(11); O(1)–Pt(1)–P(2), 91.4(2); O(4)–Pt(1)–P(1), 92.4(2).

equiv of $[(\text{DMPP})_2\text{MCl}_2]$ [$\text{M} = \text{Pd}$ (**1a**), Pt (**1b**)] in a 1:1 mixture of CH_3NO_2 and CH_3CN and filtration to remove silver chloride, 2 equiv of the dienophiles DMAA, VyPy, and DPVP were added respectively to the yellow solutions of $[(\text{DMPP})_2\text{M}(\text{CH}_3\text{CN})_2]\text{X}_2$. The reactions were monitored by $^{31}\text{P}\{^1\text{H}\}$ NMR spectroscopy, and when they were judged to be complete (several days), the solution volumes were reduced. Diethyl ether was then added to precipitate the products as microcrystalline solids. The nature of the products of these reactions (Scheme 1) is independent of the nature of the anion. However, with NO_3^- , the reactions were somewhat slower than those with the more weakly coordinating anions²⁹ and the BF_4^- salts were

generally easier to isolate and crystallize. Consequently, most of the complexes were fully characterized only as their BF_4^- salts.

Because the [4+2] Diels–Alder cycloaddition reactions all occur intramolecularly^{1–17} within the coordination sphere of the metal to form the *syn-exo*-7-phosphanorbornene skeleton (illustrated as follows), the absolute configurations of the C(1)



and C(4) stereocenters are fixed and only those at C(2) (the ring conjunction carbon) and P(7) may vary. In both of the enantiomers of these ligands, the stereochemistry of C(2) is the same as that of P(7). Thus, we will refer to the absolute configuration of these chiral ligands by a single descriptor, *R* or *S*.

Compounds **2–6** (Scheme 1) could form as either *cis*- or *trans*-geometric isomers, or as both. For **2**, **5**, and **6**, only the *cis* isomers are formed, whereas for the dienophile DPVP, both the *cis* isomers (**3**) and the *trans* isomers (**4**) are formed. The nature of the geometric isomers that are formed in these reactions may be rationalized by considering both the minimization of interligand steric interactions and the differential trans influence³⁰ of the donor atoms.

The geometric structures of the isomers were determined by a combination of ^1H , $^1\text{H}\{^{31}\text{P}\}$, $^{13}\text{C}\{^1\text{H}\}$, and $^{31}\text{P}\{^1\text{H}\}$ NMR spectroscopy of the reaction mixtures and comparison with the NMR data for the pure isolated solids. In each case, the data were the same. For **2** and **5**, single resonances in their $^{31}\text{P}\{^1\text{H}\}$ NMR spectra indicated the formation of only one geometric isomer. The small magnitudes of $^2J(\text{PP})$ values determined³¹ from the $^{13}\text{C}\{^1\text{H}\}$ NMR spectra and $^1J(\text{PtP})$ values of about 3500 Hz for the platinum complexes, determined³² from their $^{31}\text{P}\{^1\text{H}\}$ NMR spectra, are consistent with the formation of *cis* isomers (see the Experimental Section for the data).

The structures of **2** and **5** were confirmed by X-ray crystallography. Crystallographic data are listed in Table 3, and the structures are shown in Figures 3–5. All three complexes crystallize as the *cis* isomers with structures that are consistent with the NMR data. For both **2a** and **2b**, the metals lie on special positions with a crystallographic C_2 axis in the coordination plane passing through the metal atoms, which relates the two chiral ligands as illustrated in Figures 3 and 4. Thus, the two ligands bound to each metal center have the same absolute configuration and the complexes are formed as racemic mixtures of the (*R,R*) and (*S,S*) diastereomers. None of the meso (*R,S*) diastereomer is observed. Complexes **2a** and **2b** are isomorphous and isostructural with very similar M–P (2.1991(7) Å, **2a**; 2.187(2) Å, **2b**) and M–O (2.103(2) Å, **2a**; 2.091(4) Å, **2b**) distances. The M–O distances are essentially the same as those in **1a** and **1b** even though the ligands are chelating in **2a** and **2b**, which normally gives rise to a reduction in bond length relative to monodentate ligands. Both **2a** and **2b** exhibit a minor

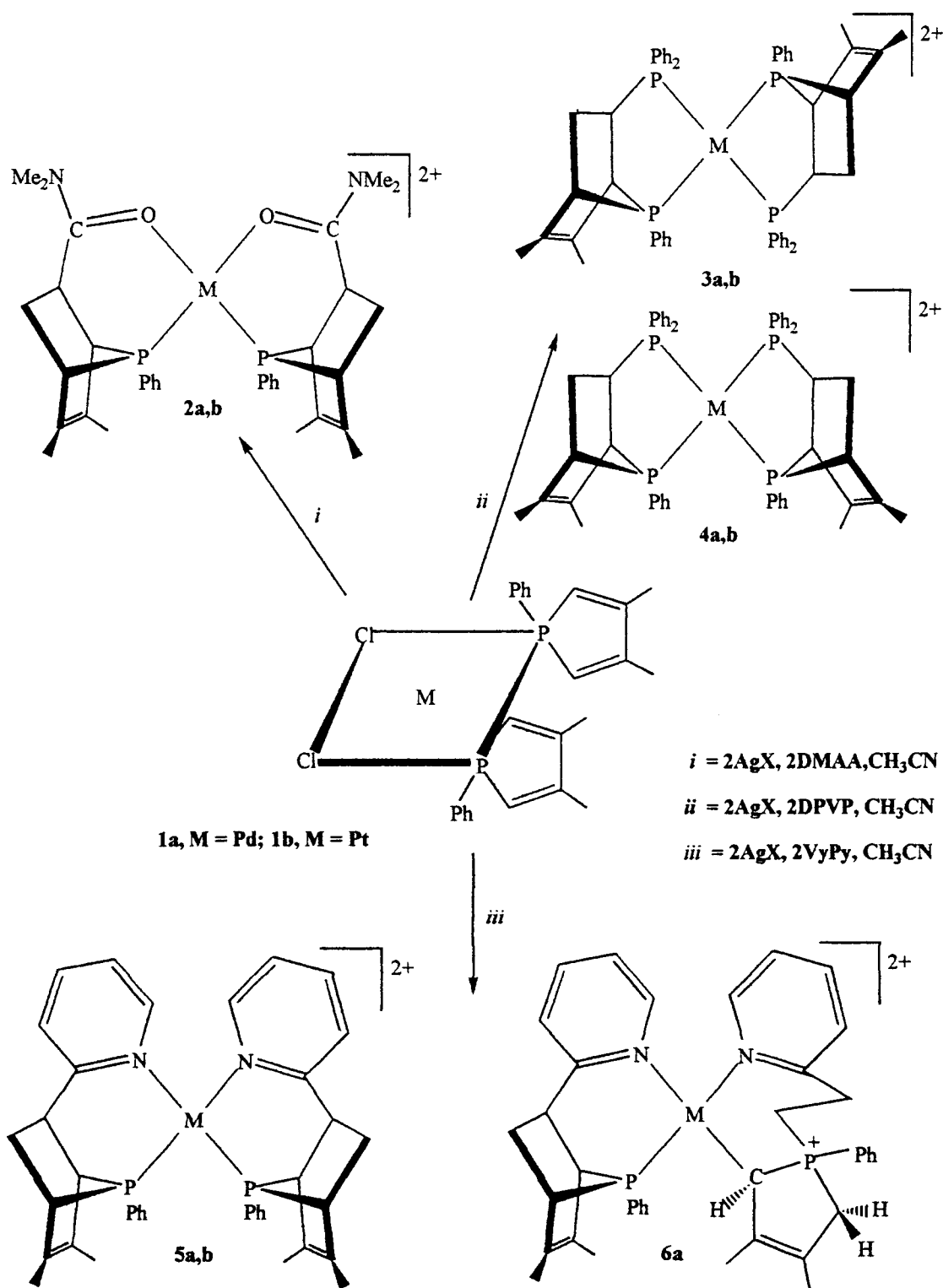
(30) Appleton, T. G.; Clark, H. C.; Manzer, L. E. *Coord. Chem. Rev.* **1973**, *10*, 335.

(31) Redfield, D. A.; Cary, L. W.; Nelson, J. H. *Inorg. Chem.* **1975**, *14*, 50.

(32) Nelson, J. H. *Coord. Chem. Rev.* **1995**, *139*, 245.

(29) Strauss, S. H. *Chem. Rev.* **1993**, *93*, 927.

Scheme 1



amount of tetrahedral distortion as indicated by the O(1)–M(1)–P(1)/O(1a)–M(1)–P(1a) dihedral angles, which are 14.5° (**2a**) and 12.6° (**2b**).

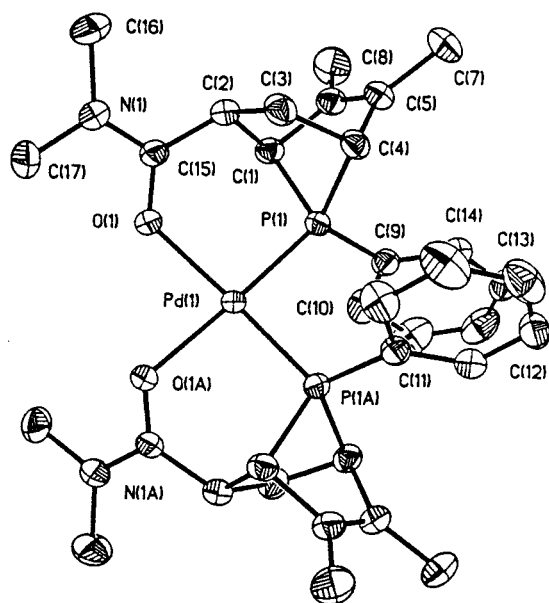
The structure of **5b** (Figure 5) shows that this compound also forms exclusively as the cis isomer, consistent with the NMR data. For this complex, as well, the two ligands are related by a crystallographic *C*₂ axis lying in the coordination plane passing through the Pt atom. Here also, a racemic mixture of the (*R,R*) and (*S,S*) diastereomers is formed. The Pt–P distances (2.238(2) Å, average) are slightly longer than those observed for **2b**, and

the Pt–N distances (2.129(5) Å, average) are longer than the Pt–O distances in **2b**. Both features probably result from slightly increased intramolecular steric interactions in **5b** compared to **2b**. The platinum coordination geometry is planar, as the sum of the angles around Pt is 360.39°.

The minor product of the reaction of [(DMPP)₂Pd(CH₃CN)₂]-X₂ with VyPy, amounting to 25% of the crude product, is **5a**. The ³¹P{¹H} NMR spectrum of the PF₆[−] salt, isolated after metathesis of the NO₃[−] salt with excess NaPF₆, exhibits a singlet at δ 72.31 and a septet at δ −145.0 (¹J(PF) = 707 Hz) in a 1:1

Table 3. Crystallographic Data for **2a**, **2b**, and **5a**

	2a	2b	5b
empirical formula	C ₃₄ H ₄₄ B ₂ F ₈ N ₂ O ₂ P ₂ Pd	C ₃₄ H ₄₄ B ₂ F ₈ N ₂ O ₂ P ₂ Pt	C ₃₈ H ₄₀ B ₂ F ₈ N ₂ P ₂ Pt·C ₃ H ₆ O
fw	854.67	943.36	1013.45
crystal system	monoclinic	monoclinic	triclinic
space group	C2/c	C2/c	P1
Z	4	4	2
a (Å)	17.973(1)	17.961(7)	10.5377(8)
b (Å)	10.6282(7)	10.583(3)	12.055(2)
c (Å)	19.741(2)	19.869(4)	19.492(2)
α (deg)	90	90	102.653(11)
β (deg)	97.789(5)	98.70(3)	97.355(7)
γ (deg)	90	90	109.097(14)
V (Å ³)	3736.2(4)	3733.0(2)	2102.4(4)
ρ _{calc} (g cm ⁻³)	1.519	1.678	1.534
T (°C)	25	25	25
μ (cm ⁻¹)	6.56	39.18	34.8
R1(F) ^a [I > 2σ(I)]	0.0440	0.0339	0.0397
wR2(F ²) ^b	0.1122	0.0762	0.0935
GOF	1.038	1.045	1.047

^a Footnote a, Table 2. ^b Footnote b, Table 2.**Figure 3.** Structural drawing of the cation of **2a**, showing the atom-numbering scheme (40% probability ellipsoids). Selected bond distances (Å) and bond angles (deg): Pd(1)–P(1), 2.1991(7); Pd(1)–O(1), 2.103(2); P(1)–Pd(1)–P(1A), 93.71(4); O(1)–Pd(1)–O(1A), 84.86(11); O(1A)–Pd(1)–P(1A), 91.66(6); O(1)–Pd(1)–P(1), 91.66(6).

integrated ratio. The ¹H and ¹³C{¹H} chemical shifts are very similar to those of the platinum analogue (**5b**), suggesting that this complex is also a racemic mixture of the (*R,R*) and (*S,S*) diastereomers with a *cis* geometry.

The ³¹P{¹H} NMR spectrum of the major isolated product of the reactions of [(DMPP)₂Pd(CH₃CN)₂]₂X₂ with VyPy, amounting to 75% of the crude product, exhibits two doublets at δ 105.35 and 38.47 (*J*(PP) = 4.9 Hz), consistent with the presence of two inequivalent coordinated phosphines with a *cis* interrelationship. The resonance at δ 105.35 is characteristic of a coordinated 7-phosphanorbornene,¹ and the resonance at δ 38.47 is typical of a phosphole coordinated to palladium.^{21,22} The ¹H and ¹³C{¹H} NMR spectra are very complicated but do not show resonances attributable to vinyl protons and carbons and to phosphole α protons and carbons. The structure of this unusual and unexpected product was established by X-ray crystallography (Figure 6). Crystallographic data are listed in

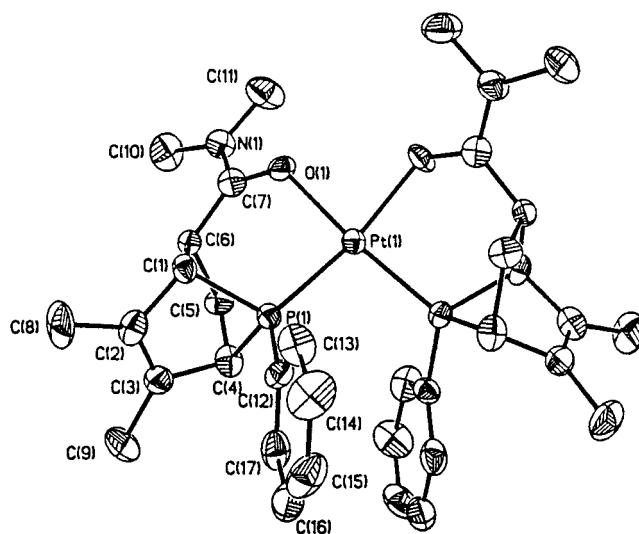
**Figure 4.** Structural drawing of the cation of **2b**, showing the atom-numbering scheme (40% probability ellipsoids). Selected bond distances (Å) and bond angles (deg): Pt(1)–P(1), 2.187(2); Pt(1)–O(1), 2.091(4); P(1)–Pt(1)–P(1A), 95.91(9); O(1)–Pt(1)–O(1A), 82.4(2); O(1A)–Pt(1)–P(1A), 91.74(13); O(1)–Pt(1)–P(1), 91.74(13).

Table 4. This compound crystallizes with two molecules of acetone in the asymmetric unit and with disordered PF₆⁻ ions. It contains a [4+2] Diels–Alder cycloadduct of VyPy and DMPP and an ylide that resulted from nucleophilic attack of a free DMPP molecule on the vinyl group of a coordinated VyPy, followed by addition of two hydrogens, probably emanating from adventitious water. The ylide is stabilized in its dipolar form by coordination of C(20) to palladium. The coordination geometry is planar; the sum of the angles around palladium is 360.4°. The two pyridine moieties are mutually *cis*, and the phosphorus and carbon donors are *cis* to one another. The metal–ligand bond lengths lie in the expected ranges. The P(2)–C(20) (1.799(7) Å) and P(2)–C(23) (1.806(4) Å) bond lengths are almost equal, so that the former is not a double bond. The C(21)–C(22) (1.333(10) Å) and C(5)–C(6) (1.332(11) Å) bond lengths are typical of carbon–carbon double bonds.

The ¹H and ¹³C{¹H} NMR spectra were then completely assigned with the aid of ¹H{³¹P}, COSY, APT, and ¹H/¹³C HETCOR experiments and were found to be consistent with the structure (see the Experimental Section for the data).

Table 4. Crystallographic Data for 6A, 3B, 4A, and 4b

	6a	3b	4a	4b
empirical formula	C ₃₈ H ₄₁ F ₁₂ N ₂ P ₄ Pd·2C ₃ H ₆ O	C ₅₂ H ₅₂ B ₂ F ₈ P ₄ Pt·C ₃ H ₆ O	C ₅₂ H ₅₂ B ₂ F ₈ P ₄ Pd·3C ₃ H ₆ O	C ₅₂ H ₅₂ B ₂ F ₈ P ₄ Pt·3C ₃ H ₆ O
fw	1100.16	1227.60	1255.07	1343.76
crystal system	triclinic	monoclinic	monoclinic	monoclinic
space group	P1	P2 ₁ /n	C2/c	C2/c
Z	2	4	4	4
a (Å)	10.384(2)	10.1466(14)	12.0940(12)	12.066(2)
b (Å)	11.912(1)	23.168(2)	26.651(4)	26.570(3)
c (Å)	21.260(2)	23.346(2)	19.298(2)	19.350(2)
α (deg)	74.937(6)	90	90	90
β (deg)	83.354(9)	91.374(9)	95.323(7)	95.197(8)
γ (deg)	84.189(9)	90	90	90
V (Å ³)	2515.3(5)	5486.5(9)	6193.3(12)	6177.8(12)
ρ _{calc} (g cm ⁻³)	1.453	1.486	1.168	1.445
T (°C)	25	25	25	25
μ (mm ⁻¹)	5.77	27.39	4.57	24.42
R1 (F) ^a [I > 2σ(I)]	0.0638	0.0739	0.0598	0.0609
wR2(F ²) ^b	0.1852	0.1136	0.1456	0.1548
GOF	0.990	1.005	1.045	1.034

^a Footnote a, Table 2. ^b Footnote b, Table 2.

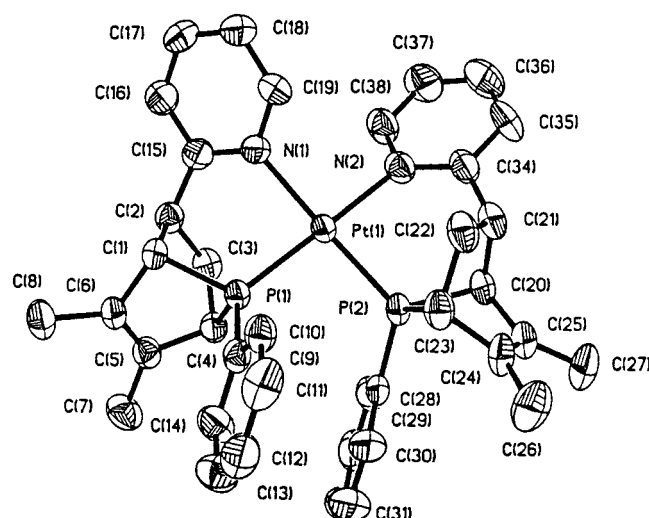


Figure 5. Structural drawing of the cation of **5b**, showing the atom-numbering scheme (40% probability ellipsoids). Selected bond distances (Å) and bond angles (deg): Pt(1)–P(1), 2.237(2); Pt(1)–P(2), 2.238(2); Pt(1)–N(1), 2.129(5); Pt(1)–N(2), 2.128(5); P(1)–Pt(1)–P(2), 92.49(6); N(1)–Pt(1)–N(2), 89.8(2); N(2)–Pt(1)–P(1), 88.3(2); N(2)–Pt(1)–P(2), 90.1(2).

The reactions of [(DMPP)₂M(CH₃CN)₂]₂X₂ with 2 equiv of DPVP produced both compounds **3** and **4**, the *cis*- and *trans*-[P₂MP₂]²⁺ species. The coordination geometry of these complexes is readily determined by ³¹P{¹H} NMR spectroscopy. The spin systems of the phosphorus nuclei for the *cis* isomers are second-order [AX]₂ spin systems, whereas those for the *trans* isomers are first-order A₂X₂ spin systems. The former give rise to a pair of centrosymmetric complex multiplets and the latter to a pair of triplets. The *cis*:*trans* ratios in the crude products, as determined by ³¹P{¹H} NMR spectroscopy, were 1.16 and 0.87 for platinum and palladium, respectively. The starting [(DMPP)₂M(CH₃CN)₂]²⁺ complexes both have the *cis* geometry in solution. Ligand substitution of CH₃CN by DPVP would be expected to occur to produce *cis*-[(DMPP)₂M(DPVP)₂]²⁺ before the Diels–Alder cycloaddition occurred. It is likely that *cis*–*trans* geometric isomerization occurs at this stage at a rate that is competitive with the rate of cycloaddition. The cycloaddition rates are expected to be nearly the same for the palladium and platinum complexes, but the isomerization rate for the palladium complexes should be faster than that for the platinum com-

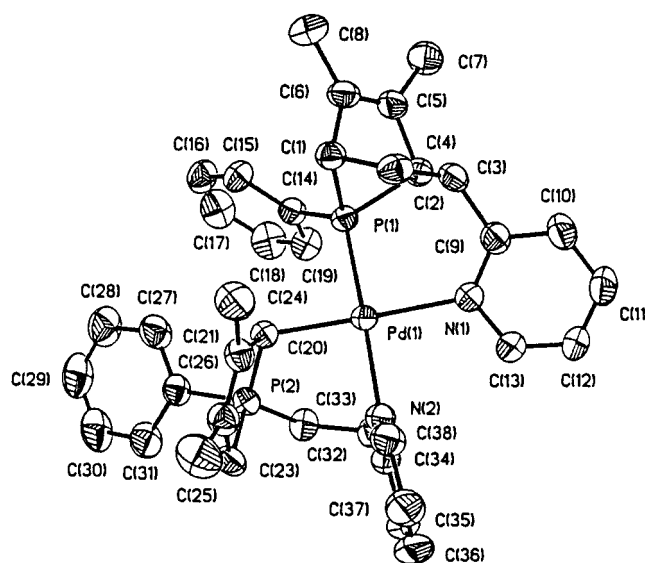


Figure 6. Structural drawing of the cation of **6a**, showing the atom-numbering scheme (40% probability ellipsoids). Selected bond distances (Å) and bond angles (deg): Pd(1)–P(1), 2.221(2); Pd(1)–N(1), 2.175(6); Pd(1)–N(2), 2.146(6); Pd(1)–C(20), 2.084(6); P(2)–C(20), 1.799(7); P(2)–C(23), 1.806(4); C(5)–C(6), 1.332(11); C(20)–C(21), 1.504(9); C(21)–C(22), 1.333(10); C(22)–C(23), 1.498(10); P(1)–Pd(1)–N(1), 91.6(2); N(1)–Pd(1)–N(2), 91.2(2); N(2)–Pd(1)–C(20), 88.7(2); C(20)–Pd(1)–P(1), 88.9(2).

plexes.^{33,34} As a result, the fraction of the *trans* isomer is greater for palladium than for platinum. The products are configurationally stable, and the geometric isomers were separated by fractional crystallization from acetone/ether mixtures, in which the *trans* isomers precipitated first.

The structures of **3b**, **4a**, and **4b** were determined by X-ray crystallography (Figures 7–9). Crystallographic data are listed in Table 4. All three compounds crystallize as acetone solvates, and all are planar, with the sums of the angles around the metals being 359.91(5), 359.98(5), and 359.88(5)°, respectively. Complex **3b** possesses a C₂ axis perpendicular to the coordination plane passing through the platinum atom. The isomorphous and isostructural complexes **4a** and **4b** possess crystallographic C₂

(33) Hartley, F. R. *The Chemistry of Platinum and Palladium*; Halsted: New York, 1973; p 313 ff.

(34) Anderson, G. K.; Cross, R. J. *Chem. Soc. Rev.* **1980**, 9, 185.

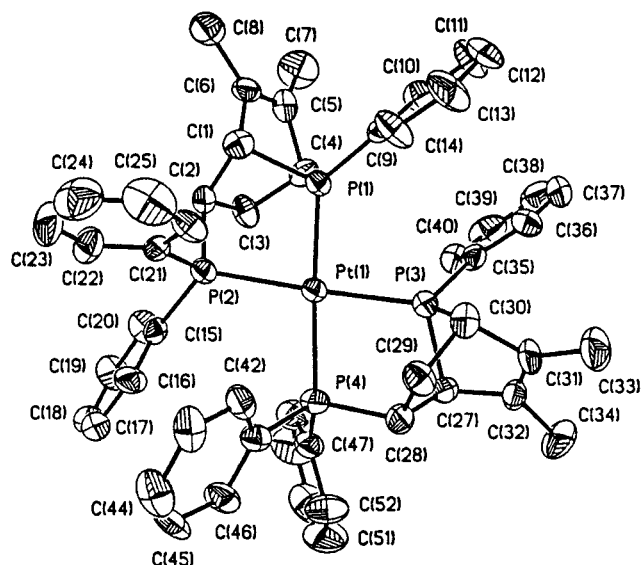


Figure 7. Structural drawing of the cation of **3b**, showing the atom-numbering scheme (40% probability ellipsoids). Selected bond distances (Å) and bond angles (deg): Pt(1)–P(1), 2.312(3); Pt(1)–P(2), 2.341(3); Pt(1)–P(3), 2.318(3); Pt(1)–P(4), 2.324(3); C(5)–C(6), 1.31(2); C(31)–C(32), 1.30(2); P(1)–Pt(1)–P(2), 81.78(11); P(1)–Pt(1)–P(3), 95.92(11); P(2)–Pt(1)–P(4), 100.34(12); P(3)–Pt(1)–P(4), 81.87(11).

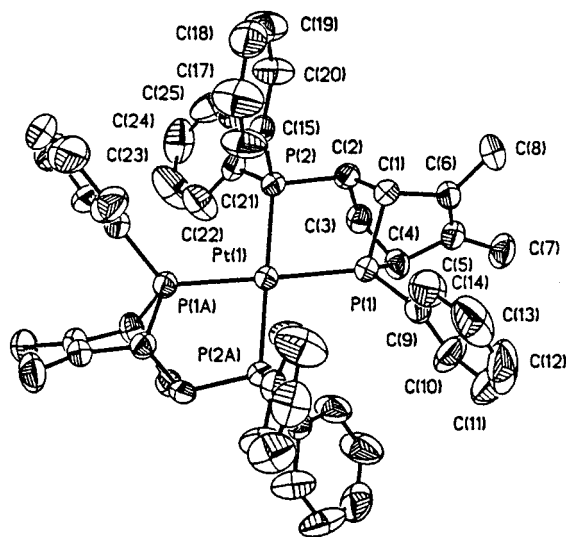


Figure 8. Structural drawing of the cation of **4b**, showing the atom-numbering scheme (40% probability ellipsoids). Selected bond distances (Å) and bond angles (deg): Pt(1)–P(1), 2.324(2); Pt(1)–P(2), 2.339(2); C(5)–C(6), 1.313(14); P(1)–Pt(1)–P(2), 81.24(7); P(1)–Pt(1)–P(2A), 98.75(7); P(1A)–Pt(1)–P(2), 98.75(7); P(1A)–Pt(1)–P(2A), 81.24(7).

axes lying in the coordination planes passing through the metal atoms. For all three complexes, these C_2 axes relate the two bidentate chiral ligands to one another. Thus, in all three cases, racemic mixtures of the (*R,R*) and (*S,S*) diastereomers are formed, and no meso (*R,S*) diastereomers are observed in the crude products. For the isomeric complexes of platinum, **3b** and **4b**, there is very little difference in the Pt–P bond lengths either within or between the complexes. This observation suggests that the two isomers have comparable thermodynamic stabilities, and in fact, the observed ratio of the isomers is near unity. A similar argument should apply to the relative thermodynamic stabilities of the analogous palladium complexes, which suggests that the isomer ratio is under kinetic control.

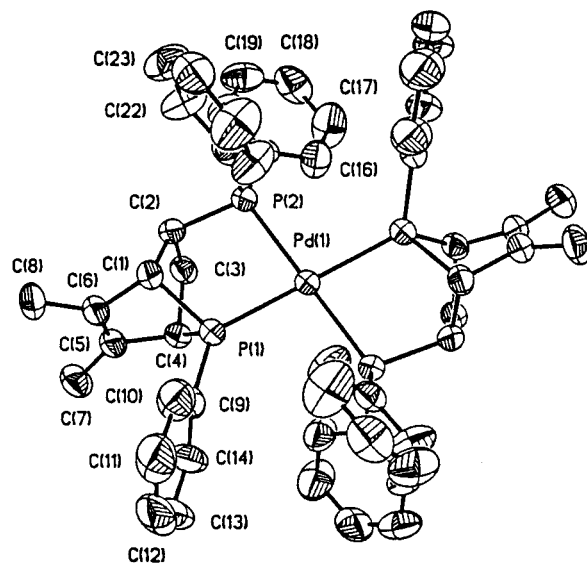


Figure 9. Structural drawing of the cation of **4a**, showing the atom-numbering scheme (40% probability ellipsoids). Selected bond distances (Å) and bond angles (deg): Pd(1)–P(1), 2.3435(13); Pd(1)–P(2), 2.350(13); C(5)–C(6), 1.328(8); P(1)–Pd(1)–P(2), 81.01(4); P(1)–Pd(1)–P(2A), 98.93(4); P(1A)–Pd(1)–P(2), 98.93(4); P(1A)–Pd(1)–P(2A), 81.01(4).

Conclusions

The complexes *cis*-[(DMPP)₂M(CH₃CN)₂]₂X₂ (M = Pd, Pt; X = NO₃[−], BF₄[−], ClO₄[−]) react with 2 equiv of the dienophiles DMAA, VyPy, and DPVP to first produce the ligand substitution products [(DMPP)₂M(dienophile)₂]₂X₂. These ligand substitution products undergo *cis*–*trans* isomerization when the dienophile is DPVP but not when the dienophile is DMAA or VyPy. The ligand substitution products then undergo two rapid sequential metal-promoted intramolecular [4+2] Diels–Alder cycloaddition reactions to produce the final products. The final products of these reactions all contain two chiral bidentate ligands. For the reactions with DMAA and VyPy, only *cis*-geometric isomers were formed. The reactions with DPVP yielded both the *cis*- and *trans*-geometric isomers. In all cases, the absolute configuration of the first Diels–Alder cycloadduct formed on the metal influenced the absolute configuration of the second Diels–Alder cycloaddition product in a complementary fashion. Racemic mixtures of the (*R,R*) and (*S,S*) diastereomers were formed, and no meso (*R,S*) diastereomers were observed. The complementarity in the fitting of the two chiral ligands around the metal center is independent of whether the two ligands are mutually *cis* or *trans*. The nature of the anion has no influence on the stereochemistry of the products.

An unusual ylide complex, **6a**, was the major product of the reaction of *cis*-[(DMPP)₂Pd(CH₃CN)₂]₂X₂ with VyPy. That none of the analogous product was observed in the reaction of *cis*-[(DMPP)₂Pt(CH₃CN)₂]₂X₂ with VyPy may be explained by the relative thermodynamic and kinetic stabilities of the palladium and platinum complexes of DMPP. The former undergo³⁵ spontaneous *cis*–*trans* isomerization in solution by a mechanism that involves dissociation of DMPP, whereas the latter do not.²³ VyPy is able to displace DMPP from palladium, but not from platinum, at some stage in the reaction, most likely after the first Diels–Alder cycloaddition. Long after submission of this paper, enantiomerically pure analogues of **2a** and **2b** were reported.³⁶

(35) MacDougall, J. J.; Mathey, F.; Nelson, J. H. *Inorg. Chem.* **1980**, *19*, 1980.

Experimental Section

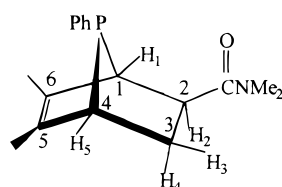
A. Reagents and Physical Measurements. All chemicals were of reagent grade and were used as received from commercial sources (Aldrich, Fisher Scientific, or Organometallics for DPVP). Elemental analyses were performed by Galbraith Laboratories, Knoxville, TN. Melting points were determined on a Mel-Temp apparatus and are uncorrected. FT-IR spectra were recorded for Nujol mulls on NaCl windows by using a Perkin-Elmer BX spectrometer. ^1H , $^1\text{H}\{^{31}\text{P}\}$, $^{13}\text{C}\{^1\text{H}\}$, and $^{31}\text{P}\{^1\text{H}\}$ NMR spectra were recorded at 499.8, 499.8, 125.7, and 202.3 MHz, respectively, on a Varian Unity Plus 500 FT-NMR spectrometer. Proton and carbon chemical shifts are relative to internal Me_4Si or solvent resonances and phosphorus chemical shifts are relative to the resonance of external 85% $\text{H}_3\text{PO}_4(\text{aq})$ with positive values being downfield of the respective reference.

B. Syntheses. **[(DMPP) $_2$ Pd(NO $_3$) $_2$] (1a).** To a solution of 0.553 g (1.00 mmol) of *cis*-[(DMPP) $_2$ PdCl $_2$] 21,22 in 25 mL of CH_3CN was added 0.340 g (2.00 mmol) of AgNO_3 . A curdy white precipitate formed immediately in a lemon-yellow solution. The mixture was stirred at ambient temperature, protected from light with aluminum foil for 1 h, and filtered to remove AgCl , after which the volume of the filtrate was reduced to 10 mL on a rotary evaporator. Ether (10 mL) was added to the solution, and the mixture was allowed to stand at ambient temperature for 4 h. The microcrystalline yellow precipitate that formed was isolated by filtration and dried under vacuum to yield 0.54 g (89%) of **1a**. Mp: 187–188 °C. Anal. Calcd for $\text{C}_{24}\text{H}_{26}\text{N}_2\text{O}_6\text{P}_2\text{Pd}$: C, 47.52; H, 4.29; N, 4.62. Found: C, 47.39; H, 4.17; N, 4.68. $^{13}\text{C}\{^1\text{H}\}$ NMR (CD_3NO_2): δ 157.69 (AXX', $^2J(\text{PC}) + ^4J(\text{PC})$) = 12.7 Hz, C_β), 132.51 (s, C_ρ), 132.41 (AXX', $^2J(\text{PC}) + ^4J(\text{PC})$) = 12.3 Hz, C_α), 129.23 (AXX', $^3J(\text{PC}) + ^5J(\text{PC})$) = 12.1 Hz, C_m), 123.12 (AXX', $^1J(\text{PC}) + ^3J(\text{PC})$) = 60.6 Hz, C_i), 119.18 (AXX', $^1J(\text{PC}) + ^3J(\text{PC})$) = 60.6 Hz, C_α), 16.66 (AXX', $^3J(\text{PC}) + ^5J(\text{PC})$) = 14.8 Hz, CH_3).

[(DMPP) $_2$ Pt(NO $_3$) $_2$] (1b). Similarly, from 0.642 g (1.00 mmol) of *cis*-[(DMPP) $_2$ PtCl $_2$] 23,24 and 0.340 g (2.00 mmol) AgNO_3 was obtained 0.58 g (90%) of colorless microcrystals of **1b**. Mp: 210–211 °C. Anal. Calcd for $\text{C}_{24}\text{H}_{26}\text{N}_2\text{O}_6\text{P}_2\text{Pt}$: C, 41.46; H, 3.74; N, 4.03. Found: C, 41.35; H, 3.68; N, 4.12. $^{13}\text{C}\{^1\text{H}\}$ NMR (CD_3NO_2): δ 157.41 (AXX', $^2J(\text{PC}) + ^4J(\text{PC})$) = 14.7 Hz, C_β), 132.42 (AXX', $^2J(\text{PC}) + ^4J(\text{PC})$) = 11.6 Hz, C_α), 132.39 (AXX', $^1J(\text{PC}) + ^6J(\text{PC})$) = 1.5 Hz, C_ρ), 129.02 (AXX', $^3J(\text{PC}) + ^5J(\text{PC})$) = 11.9 Hz, C_m), 123.47 (AXX', $^1J(\text{PC}) + ^3J(\text{PC})$) = 67.7 Hz, C_i), 119.13 (AXX', $^1J(\text{PC})$) = 63.2 Hz, $^3J(\text{PC})$ = 4.3 Hz, $^2J(\text{PP})$ = 30.8 Hz, C_α), 16.57 (AXX', $^3J(\text{PC}) + ^5J(\text{PC})$) = 15.2 Hz, CH_3).

Diels–Alder Cycloadducts. All of the cycloadducts were prepared by the same general method. To a solution containing 1.00 mmol of [(DMPP) $_2$ MCl $_2$] in 25 mL of CH_3CN and 25 mL of CH_3NO_2 was added 2.00 mmol of AgBF_4 . After the mixture was stirred for 1 h, protected from light with aluminum foil, it was filtered to remove AgCl , and 2.1 equiv of the respective dienophile was added to the filtrate. The reaction mixture was allowed to stand at ambient temperature for 4 days, the volume was reduced to 5 mL on a rotary evaporator, and ether was added to precipitate the product, which was isolated by filtration, dried under vacuum, and recrystallized from an acetone/ether mixture.

2a. Yield: 0.68 g (80%) of pale yellow crystals. Mp: 240–242 °C. IR (Nujol): $\nu_{\text{C=O}}$ 1590, 1436 cm^{-1} . The values of the aminocarbonyl CO stretching frequencies for **2a** and **2b** indicate oxygen coordination and a *cis* geometry. 37 Anal. Calcd for $\text{C}_{34}\text{H}_{44}\text{B}_2\text{F}_8\text{N}_2\text{O}_2\text{P}_2\text{Pd}$: C, 47.80; H, 5.15; N, 3.28. Found: C, 47.69; H, 5.01; N, 3.32.



$^{31}\text{P}\{^1\text{H}\}$ NMR (CD_3NO_2): δ 101.30. ^1H NMR (CD_3NO_2): δ 7.71 (m, 2H, H_ρ), 7.54 (m, 4H, H_m), 7.19 (m, 4H, H_o), 3.50 (dddd, $^3J(\text{PH})$ = 24.5 Hz, $^3J(\text{H}_2\text{H}_4)$ = 10.8 Hz, $^3J(\text{H}_2\text{H}_5)$ = 5.0 Hz, $^3J(\text{H}_1\text{H}_2)$ = 1.5 Hz, 2H, H_2), 3.31 (s, 6H, NCH_3), 3.26 (s, 6H, NCH_3), 3.24 (dd, $^3J(\text{H}_3\text{H}_5)$ = 2.5 Hz, $^3J(\text{H}_4\text{H}_5)$ = 1.0 Hz, 2H, H_5), 2.84 (d, $^3J(\text{H}_1\text{H}_2)$ = 1.5 Hz, 2H, H_1), 2.81 (dddd, $^3J(\text{H}_3\text{H}_4)$ = 13.5 Hz, $^3J(\text{PH})$ = 7.5 Hz, $^3J(\text{H}_2\text{H}_3)$ = 5.0 Hz, $^3J(\text{H}_3\text{H}_5)$ = 2.5 Hz, 2H, H_3), 2.41 (dddd, $^3J(\text{PH})$ = 37.0 Hz, $^2J(\text{H}_3\text{H}_4)$ = 13.5 Hz, $^3J(\text{H}_2\text{H}_4)$ = 10.8 Hz, $^3J(\text{H}_4\text{H}_5)$ = 1.0 Hz, 2H, H_4), 1.65 (s, 6H, CCH_3), 1.40 (s, 6H, CCH_3). $^{13}\text{C}\{^1\text{H}\}$ NMR (CD_3NO_2): δ 178.37 (s, CO), 135.42 (s, C_α or C_5), 134.25 (s, C_5 or C_6), 133.29 (AXX', $^2J(\text{PC}) + ^4J(\text{PC})$) = 11.3 Hz, C_α), 133.24 (s, C_ρ), 129.19 (AXX', $^3J(\text{PC})$ = 10.5 Hz, $^5J(\text{PC})$ = 0.4 Hz, $^2J(\text{PP})$ = 8.3 Hz, C_m), 122.49 (AXX', $^1J(\text{PC})$ = 57.8 Hz, $^3J(\text{PC})$ = 3.6 Hz, C_i), 49.22 (AXX', $^1J(\text{PC})$ = 36.1 Hz, $^3J(\text{PC})$ = 2.6 Hz, C_i), 45.63 (AXX', $^1J(\text{PC})$ = 37.6 Hz, $^3J(\text{PC})$ = 2.3 Hz, C_4), 39.67 (AXX', $^2J(\text{PC})$ = 17.6 Hz, $^4J(\text{PC})$ = 1.2 Hz, $^2J(\text{PP})$ = 8.3 Hz, C_2), 37.95 (s, NCH_3), 36.70 (s, NCH_3), 30.09 (AXX', $^2J(\text{PC})$ = 25.2 Hz, $^4J(\text{PC})$ = 0.5 Hz, $^2J(\text{PP})$ = 8.3 Hz, C_3), 12.78 (AXX', $^3J(\text{PC}) + ^5J(\text{PC})$) = 3.6 Hz, CCH_3), 12.59 (AXX', $^3J(\text{PC}) + ^5J(\text{PC})$) = 2.8 Hz, CCH_3).

2b. Yield: 0.80 g (85%) of colorless crystals. Mp: 273–275 °C. IR (Nujol): $\nu_{\text{C=O}}$ 1583, 1456 cm^{-1} . Anal. Calcd for $\text{C}_{34}\text{H}_{44}\text{B}_2\text{F}_8\text{N}_2\text{O}_2\text{Pt}$: C, 43.30; H, 4.67; N, 2.97. Found: C, 43.16; H, 4.71; N, 3.02. $^{31}\text{P}\{^1\text{H}\}$ NMR (CD_3NO_2): δ 74.4, $^1J(\text{PtP})$ = 3560 Hz. ^1H NMR (CD_3NO_2): δ 7.66 (m, 2H, H_ρ), 7.49 (m, 4H, H_m), 7.13 (m, 2H, H_o), 3.50 (dddd, $^3J(\text{PH})$ = 22.0 Hz, $^3J(\text{H}_2\text{H}_4)$ = 10.5 Hz, $^3J(\text{H}_2\text{H}_5)$ = 4.5 Hz, $^3J(\text{H}_1\text{H}_2)$ = 1.0 Hz, 2H, H_2), 3.37 (s, 6H, NCH_3), 3.33 (s, 6H, NCH_3), 3.19 (apparent t, $^2J(\text{PH})$ = $^3J(\text{H}_2\text{H}_5)$ = 1.5 Hz, 2H, H_5), 2.97 (apparent t, $^2J(\text{PH})$ = $^3J(\text{H}_1\text{H}_2)$ = 1.0 Hz, 2H, H_1), 2.83 (apparent ddt, $^2J(\text{H}_3\text{H}_4)$ = 13.0 Hz, $^3J(\text{H}_2\text{H}_3)$ = 4.5 Hz, $^3J(\text{PH})$ = $^3J(\text{H}_3\text{H}_5)$ = 1.5 Hz, 2H, H_3), 2.29 (dddd, $^3J(\text{PH})$ = 35.5 Hz, $^2J(\text{H}_3\text{H}_4)$ = 13.0 Hz, $^3J(\text{H}_2\text{H}_4)$ = 10.5 Hz, $^3J(\text{H}_4\text{H}_5)$ = 1.5 Hz, 2H, H_4), 1.67 (s, 6H, CCH_3), 1.40 (s, 6H, CCH_3). $^{13}\text{C}\{^1\text{H}\}$ NMR (CD_3NO_2): δ 179.03 (s, CO), 135.05 (s, C_α or C_5), 133.12 (s, C_ρ), 133.06 (AXX', $^2J(\text{PC})$ = 12.1 Hz, $^4J(\text{PC})$ = -1.8 Hz, $^2J(\text{PP})$ = 10.7 Hz, C_α), 132.86 (AXX', $^2J(\text{PC}) + ^4J(\text{PC})$) = 1.9 Hz, C_5 or C_6), 129.01 (AXX', $^3J(\text{PC})$ = 10.7 Hz, $^5J(\text{PC})$ = -0.6 Hz, $^2J(\text{PP})$ = 10.7 Hz, C_m), 122.26 (AXX', $^1J(\text{PC}) + ^3J(\text{PC})$) = 70.0 Hz, C_i), 47.29 (AXX', $^1J(\text{PC})$ = 40.5 Hz, $^3J(\text{PC})$ = -1.2 Hz, $^2J(\text{PP})$ = 10.7 Hz, C_4), 44.86 (AXX', $^1J(\text{PC})$ = 42.7 Hz, $^3J(\text{PC})$ = -0.3 Hz, $^2J(\text{PP})$ = 10.7 Hz, C_1), 39.85 (AXX', $^2J(\text{PC})$ = 15.6 Hz, $^4J(\text{PC})$ = -0.7 Hz, $^2J(\text{PP})$ = 10.7 Hz, C_2), 38.47 (AXX', $^5J(\text{PC}) + ^7J(\text{PC})$) = 3.3 Hz, NCH_3), 37.35 (AXX', $^5J(\text{PC}) + ^7J(\text{PC})$) = 2.9 Hz, NCH_3), 30.11 (AXX', $^2J(\text{PC})$ = 22.4 Hz, $^4J(\text{PC})$ = -0.1 Hz, $^2J(\text{PP})$ = 10.7 Hz, C_3), 12.50 (AXX', $^3J(\text{PC}) + ^5J(\text{PC})$) = 4.3 Hz, CCH_3), 12.33 (AXX', $^3J(\text{PC}) + ^5J(\text{PC})$) = 3.5 Hz, CCH_3).

3a. This compound could not be isolated in isomerically pure form. Consequently, the following NMR spectral data are assigned from the NMR spectra of *cis* and *trans* mixtures. $^{31}\text{P}\{^1\text{H}\}$ (CD_3NO_2): δ 112.95 (P_A), 35.04 (P_X), $^2J(\text{AX}') = ^2J(\text{A}'\text{X}) = 278.1$ Hz, $^2J(\text{AA}') = ^2J(\text{XX}') = 11.2$ Hz, $^2J(\text{AX}) = ^2J(\text{A}'\text{X}) = 36.9$ Hz. ^1H NMR (CD_3NO_2): δ 6.8–7.9 (m, 30H, Ph), 3.56 (m, 2H, H_2), 3.52 (m, 2H, H_5), 3.18 (m, 2H, H_1), 2.94 (m, 2H, H_3), 2.42 (m, 2H, H_4), 1.81 (s, 6H, CH_3), 1.36 (s, 6H, CH_3).

3b. Yield: 0.42 g (36%) of colorless crystals. Mp: 174–175 °C. Anal. Calcd for $\text{C}_{52}\text{H}_{52}\text{B}_2\text{F}_8\text{P}_4\text{Pt}$: C, 53.42; H, 4.45. Found: C, 53.28; H, 4.29. $^{31}\text{P}\{^1\text{H}\}$ NMR (CD_3NO_2): δ 101.18 (P_A), $^1J(\text{PtP})$ = 2114 Hz), 30.13 (P_X), $^1J(\text{PtP})$ = 2250 Hz), $^2J(\text{AX}') = ^2J(\text{A}'\text{X}) = 270.9$ Hz, $^2J(\text{AA}') = 17.3$ Hz, $^2J(\text{XX}') = 11.1$ Hz, $^2J(\text{AX}) = ^2J(\text{A}'\text{X}) = -23.8$ Hz. ^1H NMR (CD_3NO_2): δ 7.1–7.7 (m, 30H, Ph), 3.65 (m, 2H, H_2), 3.56 (m, 2H, H_5), 3.02 (m, 2H, H_1), 3.00 (m, 2H, H_3), 2.29 (m, 2H, H_4), 1.84 (s, 6H, CH_3), 1.34 (s, 6H, CH_3). $^{13}\text{C}\{^1\text{H}\}$ NMR (CD_3NO_2): δ 136.47 ($\text{AA}'\text{MM}'\text{X}$, $^3J(\text{PC})$ = 24.9 Hz, $^2J(\text{PC}) + ^4J(\text{PC})$) = 1.4 Hz, C_α), 135.05 ($\text{AA}'\text{MM}'\text{X}$, $^2J(\text{PC}) + ^4J(\text{PC})$) = 11.7 Hz, C_α), 133.50 (s, C_ρ), 133.46 ($\text{AA}'\text{MM}'\text{X}$, $^2J(\text{PC}) + ^4J(\text{PC})$) = 9.6 Hz, C_α), 132.98 (s, C_ρ), 132.79 (s, C_ρ), 132.34 ($\text{AA}'\text{MM}'\text{X}$, $^2J(\text{PC}) + ^4J(\text{PC})$) = 10.8 Hz, C_α), 129.75 ($\text{AA}'\text{MM}'\text{X}$, $^3J(\text{PC}) + ^5J(\text{PC})$) = 11.2 Hz, C_m), 129.39 ($\text{AA}'\text{MM}'\text{X}$, $^3J(\text{PC}) + ^5J(\text{PC})$) = 11.2 Hz, C_m), 129.28 ($\text{AA}'\text{MM}'\text{X}$, $^3J(\text{PC}) + ^5J(\text{PC})$) = 11.2 Hz, C_m), 128.14 ($\text{AA}'\text{MM}'\text{X}$, $^2J(\text{PC}) + ^4J(\text{PC})$) = 17.5 Hz, C_5), 125.50 ($\text{AA}'\text{MM}'\text{X}$, $^1J(\text{PC}) + ^3J(\text{PC})$) = 55.7

(36) Leung, P.-H.; He, G.; Lang, H.; Liu, A.; Loh, S.-K.; Selvaratnam, S.; Mok, K. F.; White, A. J. P.; Williams, D. J. *Tetrahedron* **2000**, 56, 7.

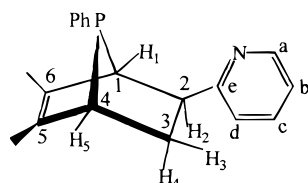
(37) James, B. R.; Ochaiai, E.; Rempel, J. L. *Inorg. Nucl. Chem. Lett.* **1971**, 7, 781.

Hz, C_i), 124.82 (AA'MM'X, $|^1J(\text{PC}) + ^3J(\text{PC})| = 54.7$ Hz, C_i), 123.20 (AA'MM'X, $|^1J(\text{PC}) + ^3J(\text{PC})| = 54.2$ Hz, C_i), 54.69 (AA'MM'X, $|^1J(\text{PC}) + ^3J(\text{PC})| = 38.5$ Hz, C_i), 47.54 (AA'MM'X, $|^1J(\text{PC}) + ^3J(\text{PC})| = 36.2$ Hz, C₂), 33.84 (AA'MM'X, $|^1J(\text{PC}) + ^3J(\text{PC})| = 35.2$ Hz, C₄), 31.92 (AA'MM'X, $|^2J(\text{PC}) + ^4J(\text{PC})| = 16.8$ Hz, C₃), 13.04 (AA'MM'X, $|^3J(\text{PC}) + ^5J(\text{PC})| = 2.6$ Hz, CH₃), 12.11 (AA'MM'X, $|^3J(\text{PC}) + ^5J(\text{PC})| = 3.3$ Hz, CH₃).

4a. Yield: 0.37 g (34%) of pale yellow crystals. Mp: 189–191 °C. Anal. Calcd for C₅₂H₅₂B₂F₈P₄Pd: C, 57.81; H, 4.81. Found: C, 57.59; H, 4.64. $^{31}\text{P}\{^1\text{H}\}$ NMR (CD₃NO₂): δ 116.96 (t, P_A), 33.90 (t, P_X), $^2J(\text{AX}) = 24.0$ Hz. ^1H NMR (CD₃NO₂): δ 6.8–7.9 (m, 30H, Ph), 3.76 (s, 2H, H₅), 3.56 (m, 2H, H₂), 3.46 (s, 2H, H₁), 3.01 (m, 2H, H₃), 2.18 (m, 2H, H₄), 1.60 (s, 6H, CH₃), 1.46 (s, 6H, CH₃). $^{13}\text{C}\{^1\text{H}\}$ NMR (CD₃NO₂): δ 137.56 (AA'MM'X, $|^2J(\text{PC}) + ^4J(\text{PC})| = 1.3$ Hz, C₆), 134.65 (AA'MM'X, $|^2J(\text{PC}) + ^4J(\text{PC})| = 13.3$ Hz, C₀), 133.94 (AA'MM'X, $|^2J(\text{PC}) + ^4J(\text{PC})| = 13.1$ Hz, C₀), 133.51 (s, C_p), 133.43 (s, C_p), 131.89 (s, C_p), 131.77 (AA'MM'X, $|^2J(\text{PC}) + ^4J(\text{PC})| = 10.2$ Hz, C₀), 130.68 (AA'MM'X, $|^2J(\text{PC}) + ^4J(\text{PC})| = 17.5$ Hz, C₅), 129.97 (AA'MM'X, $|^3J(\text{PC}) + ^5J(\text{PC})| = 11.7$ Hz, C_m), 129.92 (AA'MM'X, $|^3J(\text{PC}) + ^5J(\text{PC})| = 11.8$ Hz, C_m), 128.81 (AA'MM'X, $|^3J(\text{PC}) + ^5J(\text{PC})| = 10.1$ Hz, C_m), 126.36 (AA'MM'X, $|^1J(\text{PC}) + ^3J(\text{PC})| = 50.3$ Hz, C_i), 124.45 (AA'MM'X, $|^1J(\text{PC}) + ^3J(\text{PC})| = 46.1$ Hz, C_i), 122.35 (AA'MM'X, $|^1J(\text{PC}) + ^3J(\text{PC})| = 52.0$ Hz, C_i), 55.29 (AA'MM'X, $|^1J(\text{PC}) + ^3J(\text{PC})| = 28.9$ Hz, C₂), 33.76 (AA'MM'X, $|^1J(\text{PC}) + ^3J(\text{PC})| = 38.8$ Hz, C₄), 29.80 (AA'MM'X, $|^2J(\text{PC}) + ^4J(\text{PC})| = 17.8$ Hz, C₃), 13.30 (s, CH₃), 12.35 (s, CH₃).

4b. Yield: 0.29 g (25%) of pale yellow crystals. Mp: 210–212 °C. Anal. Calcd for C₅₂H₅₂B₂F₈P₄Pt: C, 53.42; H, 4.75. Found: C, 53.56; H, 4.54. $^{31}\text{P}\{^1\text{H}\}$ NMR (CD₃NO₂): δ 104.58 (t, $^1J(\text{PtP}) = 2048$ Hz, P_A), 27.13 (t, $^1J(\text{PtP}) = 2405$ Hz, $^3J(\text{P}_A\text{P}_X) = 19.5$ Hz, P_X), ^1H NMR (CD₃NO₂): δ 6.7–7.9 (m, 30H, Ph), 3.73 (s, 2H, H₅), 3.65 (m, 2H, H₂), 3.29 (s, 2H, H₁), 2.97 (m, 2H, H₃), 2.07 (m, 2H, H₄), 1.60 (s, 6H, CH₃), 1.43 (s, 6H, CH₃). $^{13}\text{C}\{^1\text{H}\}$ NMR (CD₃NO₂): δ 138.96 (AA'MM'X, $^3J(\text{PtC}) = 24.3$ Hz, $|^2J(\text{PC}) + ^4J(\text{PC})| = 1.4$ Hz, C₆), 136.30 (AA'MM'X, $|^2J(\text{PC}) + ^4J(\text{PC})| = 13.2$ Hz, C₀), 135.54 (AA'MM'X, $|^2J(\text{PC}) + ^4J(\text{PC})| = 12.6$ Hz, C₀), 135.28 (s, C_p), 135.00 (s, C_p), 133.39 (s, C_p), 133.18 (AA'MM'X, $|^2J(\text{PC}) + ^4J(\text{PC})| = 12.5$ Hz, C₀), 131.50 (AA'MM'X, $|^3J(\text{PC}) + ^5J(\text{PC})| = 11.4$ Hz, C_m), 131.35 (AA'MM'X, $|^3J(\text{PC}) + ^5J(\text{PC})| = 11.2$ Hz, C_m), 130.66 (AA'MM'X, $|^2J(\text{PC}) + ^4J(\text{PC})| = 15.7$ Hz, C₅), 130.15 (AA'MM'X, $|^3J(\text{PC}) + ^5J(\text{PC})| = 10.4$ Hz, C_m), 127.32 (AA'MM'X, $|^1J(\text{PC}) + ^3J(\text{PC})| = 58.1$ Hz, C_i), 124.77 (AA'MM'X, $|^1J(\text{PC}) + ^3J(\text{PC})| = 56.2$ Hz, C_i), 123.44 (AA'MM'X, $|^1J(\text{PC}) + ^3J(\text{PC})| = 59.8$ Hz, C_i), 56.05 (AA'MM'X, $|^1J(\text{PC}) + ^3J(\text{PC})| = 40.0$ Hz, C₁), 50.92 (AA'MM'X, $|^1J(\text{PC}) + ^3J(\text{PC})| = 34.8$ Hz, C₂), 34.82 (AA'MM'X, $|^1J(\text{PC}) + ^3J(\text{PC})| = 35.7$ Hz, C₄), 31.30 (AA'MM'X, $|^2J(\text{PC}) + ^4J(\text{PC})| = 18.9$ Hz, C₃), 14.71 (AA'MM'X, $|^3J(\text{PC}) + ^5J(\text{PC})| = 2.1$ Hz, CH₃), 13.70 (AA'MM'X, $|^3J(\text{PC}) + ^5J(\text{PC})| = 2.9$ Hz, CH₃).

5a. This compound was isolated as the PF₆[−] salt obtained by metathesis of the NO₃[−] product with excess NaPF₆ in CH₃NO₂. Yield: 0.18 g (18%) of pale yellow microcrystals. Mp: 186–187 °C. Anal. Calcd for C₃₈H₄₀F₁₂N₂P₄Pd: C, 46.44; H, 4.07; N, 2.85. Found: C, 46.29; H, 3.88; N, 2.67.

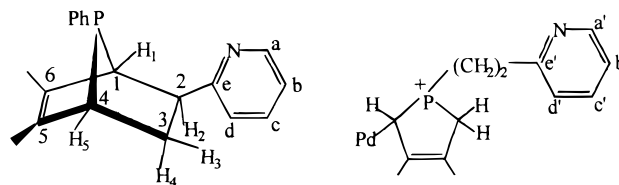


$^{31}\text{P}\{^1\text{H}\}$ NMR (CD₃NO₂): δ 72.31, −145.00 (septet, $^1J(\text{PF}) = 707$ Hz). ^1H NMR (CD₃NO₂): δ 8.76 (dd, $^3J(\text{H}_a\text{H}_b) = 6.0$ Hz, $^4J(\text{H}_a\text{H}_c) = 1.5$ Hz, 2H, H_a), 8.52 (apparent td, $^3J(\text{H}_b\text{H}_c) = ^3J(\text{H}_c\text{H}_d) = 7.5$ Hz, $^4J(\text{H}_a\text{H}_c) = 1.5$ Hz, 2H, H_c), 8.01 (dd, $^3J(\text{H}_c\text{H}_d) = 7.5$ Hz, $^4J(\text{H}_b\text{H}_d) = 1.0$ Hz, 2H, H_d), 7.96 (ddd, $^3J(\text{H}_b\text{H}_c) = 7.5$ Hz, $^3J(\text{H}_a\text{H}_b) = 6.0$ Hz, $^4J(\text{H}_b\text{H}_d) = 1.0$ Hz, 2H, H_b), 7.83 (m, 4H, H₀), 7.69 (m, 2H, H_p), 7.59 (m, 4H, H_m), 3.58 (dddd, $^3J(\text{PH}) = 21.0$ Hz, $^3J(\text{H}_2\text{H}_4) = 10.8$ Hz, $^3J(\text{H}_2\text{H}_3) = 6.3$ Hz, $^3J(\text{H}_1\text{H}_2) = 1.0$ Hz, 2H, H₂), 3.45 (apparent dtd, $^2J(\text{PH}) = 7.0$ Hz, $^3J(\text{H}_3\text{H}_5) = ^3J(\text{H}_4\text{H}_5) = 2.5$ Hz, $^4J(\text{H}_1\text{H}_3) = 2.0$ Hz,

2H, H₅), 3.41 (ddd, $^2J(\text{PH}) = 4.5$ Hz, $^4J(\text{H}_1\text{H}_3) = 2.0$ Hz, $^3J(\text{H}_1\text{H}_2) = 1.0$ Hz, 2H, H₁), 2.75 (dddd, $^3J(\text{PH}) = 29.0$ Hz, $^2J(\text{H}_3\text{H}_4) = 13.5$ Hz, $^3J(\text{H}_2\text{H}_4) = 10.8$ Hz, $^3J(\text{H}_4\text{H}_5) = 2.5$ Hz, 2H, H₄), 2.63 (apparent dtd, $^2J(\text{H}_3\text{H}_4) = 13.5$ Hz, $^2J(\text{H}_2\text{H}_3) = 6.3$ Hz, $^3J(\text{H}_3\text{H}_5) = ^3J(\text{PH}) = 2.5$ Hz, 2H, H₃), 1.78 (dq, $^4J(\text{PH}) = ^5J(\text{HH}) = 1.0$ Hz, 6H, CH₃), 1.74 (dq, $^4J(\text{PH}) = 2.0$ Hz, $^5J(\text{HH}) = 1.0$ Hz, 6H, CH₃). $^{13}\text{C}\{^1\text{H}\}$ NMR (CD₃NO₂): δ 160.22 (C_e), 148.51 (C_a), 144.11 (C_c), 135.95 (d, $^2J(\text{PC}) = 8.3$ Hz, C₅ or C₆), 135.65 (d, $^2J(\text{PC}) = 10.4$ Hz, C₅ or C₆), 134.87 (d, $^4J(\text{PC}) = 2.8$ Hz, C_p), 133.43 (d, $^2J(\text{PC}) = 9.1$ Hz, C₀), 130.98 (d, $^3J(\text{PC}) = 12.2$ Hz, C_m), 130.40 (C_d), 127.37 (C_b), 127.16 (d, $^1J(\text{PC}) = 103.6$ Hz, C_i), 51.44 (d, $^1J(\text{PC}) = 64.6$ Hz, C_i), 48.21 (d, $^1J(\text{PC}) = 64.2$ Hz, C₄), 46.42 (d, $^2J(\text{PC}) = 16.0$ Hz, C₂), 35.29 (d, $^2J(\text{PC}) = 13.6$ Hz, C₃), 15.22 (d, $^3J(\text{PC}) = 5.2$ Hz, CH₃), 14.69 (d, $^3J(\text{PC}) = 4.5$ Hz, CH₃).

5b. Yield: 0.72 g (75%) of colorless crystals. Mp: 233–235 °C. Anal. Calcd for C₃₈H₄₀B₂F₈N₂P₂Pt: C, 47.79; H, 4.68; N, 2.93. Found: C, 47.65; H, 4.57; N, 2.84. $^{31}\text{P}\{^1\text{H}\}$ NMR (CD₃NO₂): δ 66.25, $^1J(\text{PtP}) = 2975$ Hz. ^1H NMR (CD₃NO₂): δ 8.19 (apparent td, $^3J(\text{H}_b\text{H}_c) = ^3J(\text{H}_c\text{H}_d) = 7.5$ Hz, $^4J(\text{H}_a\text{H}_c) = 1.5$ Hz, 2H, H_c), 8.00 (dd, $^3J(\text{H}_b\text{H}_c) = 5.8$ Hz, $^4J(\text{H}_a\text{H}_c) = 1.5$ Hz, 2H, H_a), 7.81 (dd, $^3J(\text{H}_c\text{H}_d) = 7.5$ Hz, $^4J(\text{H}_b\text{H}_d) = 1.5$ Hz, 2H, H_d), 7.69 (m, 2H, H_p), 7.49 (m, 4H, H_m), 7.46 (ddd, $^3J(\text{H}_b\text{H}_c) = 7.5$ Hz, $^3J(\text{H}_a\text{H}_b) = 5.8$ Hz, $^4J(\text{H}_b\text{H}_d) = 1.5$ Hz, 2H, H_b), 7.10 (b m, 4H, H₀), 3.74 (dddd, $^3J(\text{PH}) = 24.0$ Hz, $^2J(\text{H}_2\text{H}_4) = 10.8$ Hz, $^3J(\text{H}_2\text{H}_3) = 4.5$ Hz, $^3J(\text{H}_1\text{H}_2) = 0.5$ Hz, 2H, H₂), 3.63 (apparent dtd, $^2J(\text{H}_3\text{H}_4) = 13.3$ Hz, $^3J(\text{H}_2\text{H}_3) = 4.5$ Hz, $^3J(\text{PH}) = ^3J(\text{H}_3\text{H}_5) = 2.3$ Hz, 2H, H₃), 3.23 (apparent dq, $^3J(\text{H}_3\text{H}_5) = 2.3$ Hz, $^2J(\text{PH}) = ^4J(\text{H}_1\text{H}_3) = ^3J(\text{H}_4\text{H}_5) = 1.5$ Hz, 2H, H₅), 2.84 (apparent td, $^2J(\text{PH}) = ^4J(\text{H}_1\text{H}_3) = 1.5$ Hz, $^3J(\text{H}_1\text{H}_2) = 0.5$ Hz, 2H, H₁), 2.56 (dddd, $^3J(\text{PH}) = 35.5$ Hz, $^2J(\text{H}_3\text{H}_4) = 13.3$ Hz, $^2J(\text{H}_2\text{H}_4) = 10.8$ Hz, $^3J(\text{H}_4\text{H}_5) = 1.5$ Hz, 2H, H₄), 1.78 (q, $^5J(\text{HH}) = 0.5$ Hz, 6H, CH₃), 1.41 (q, $^5J(\text{HH}) = 0.5$ Hz, 6H, CH₃). $^{13}\text{C}\{^1\text{H}\}$ NMR (CD₃NO₂): δ 163.86 (C_e), 153.40 (d, $^3J(\text{PC}) = 2.5$ Hz, C_a), 142.21 (C_c), 133.96 (C₅ or C₆), 133.28 (AXX', $|^2J(\text{PC}) + ^4J(\text{PC})| = 9.9$ Hz, C₀), 133.02 (C_p), 132.34 (C₅ or C₆), 128.99 (AXX', $^3J(\text{PC}) = 12.3$ Hz, $^5J(\text{PC}) = -1.5$ Hz, $^2J(\text{PP}) = 14.0$ Hz, C_m), 128.43 (C_d), 125.24 (C_b), 120.45 (AXX', $|^1J(\text{PC}) + ^3J(\text{PC})| = 63.1$ Hz, C_i), 50.14 (AXX', $|^1J(\text{PC}) + ^3J(\text{PC})| = 40.2$ Hz, C₁), 47.14 (AXX', $|^1J(\text{PC}) + ^3J(\text{PC})| = 48.1$ Hz, C₄), 46.31 (AXX', $^2J(\text{PC}) = 14.2$ Hz, $^4J(\text{PC}) = 3.1$ Hz, $^2J(\text{PP}) = 14.0$ Hz, C₂), 34.37 (AXX', $^2J(\text{PC}) = 24.7$ Hz, $^4J(\text{PC}) = 0.4$ Hz, $^2J(\text{PP}) = 14.0$ Hz, C₃), 12.54 (AXX', $|^3J(\text{PC}) + ^5J(\text{PC})| = 1.1$ Hz, CH₃), 12.35 (AXX', $|^3J(\text{PC}) + ^5J(\text{PC})| = 3.6$ Hz, CH₃).

6a. Yield: 0.48 g (55%) of pale yellow crystals. Mp: 205–207 °C. Anal. Calcd for C₃₈H₄₂B₂F₈N₂P₃Pd: C, 52.56; H, 4.84; N, 3.23. Found: C, 52.43; H, 4.67; N, 3.14.



$^{31}\text{P}\{^1\text{H}\}$ NMR (CD₃NO₂): δ 105.35 (d, P₇), 38.47 (d, ^+P , $J(\text{PP}) = 4.9$ Hz). ^1H NMR (CD₃NO₂): δ 8.42 (dd, $^3J(\text{H}_a\text{H}_b) = 6.0$ Hz, $^4J(\text{H}_a\text{H}_c) = 1.5$ Hz, 1H, H_a'), 8.23 (apparent td, $^3J(\text{H}_c\text{H}_d) = ^3J(\text{H}_b\text{H}_c) = 7.5$ Hz, $^4J(\text{H}_a\text{H}_c) = 1.5$ Hz, 1H, H_c'), 7.96 (apparent td, $^3J(\text{H}_c\text{H}_d) = ^3J(\text{H}_b\text{H}_c) = 7.5$ Hz, $^4J(\text{H}_a\text{H}_c) = 1.5$ Hz, 1H, H_c'), 7.88 (dd, $^3J(\text{H}_c\text{H}_d) = 7.5$ Hz, $^4J(\text{H}_b\text{H}_d) = 1.0$ Hz, 1H, H_d'), 7.80 (m, 2H, H₀), 7.71 (ddd, $^3J(\text{H}_b\text{H}_c) = 7.5$ Hz, $^3J(\text{H}_a\text{H}_b) = 6.0$ Hz, $^4J(\text{H}_b\text{H}_d) = 1.0$ Hz, 1H, H_b'), 7.64 (dd, $^3J(\text{H}_c\text{H}_d) = 7.5$ Hz, $^4J(\text{H}_b\text{H}_d) = 1.5$ Hz, 1H, H_d), 7.62 (m, 1H, H_p), 7.51 (dd, $^3J(\text{H}_a\text{H}_b) = 6.0$ Hz, $^4J(\text{H}_a\text{H}_c) = 1.5$ Hz, 1H, H_a), 7.42 (m, 5H, H_m, H_p), 7.18 (ddd, $^3J(\text{H}_b\text{H}_c) = 7.5$ Hz, $^3J(\text{H}_a\text{H}_b) = 6.0$ Hz, $^4J(\text{H}_b\text{H}_d) = 1.5$ Hz, 1H, H_b), 7.00 (m, 2H, H₀), 4.97 (dddd, $^2J(\text{PH}) = 14.0$ Hz, $^4J(\text{HH}) = 10.8$ Hz, $^4J(\text{HH}) = 7.3$ Hz, $^2J(\text{PH}) = 3.0$ Hz, 1H, P⁺CH₂), 4.20 (dddd, $^2J(\text{PH}) = 35.0$ Hz, $^2J(\text{HH}) = 14.0$ Hz, $^4J(\text{HH}) = 8.0$ Hz, $^4J(\text{HH}) = 1.5$ Hz, 1H, P⁺CH₂), 3.94 (apparent dtd, $^3J(\text{H}_3\text{H}_5) = 2.0$ Hz, $^3J(\text{H}_4\text{H}_5) = ^4J(\text{H}_1\text{H}_3) = 1.5$ Hz, 2J , $^3J(\text{H}_1\text{H}_2) = 1.5$ Hz, 1H, H₂), 3.36 (dddd, $^2J(\text{H}_3\text{H}_4) = 13.5$ Hz, $^3J(\text{H}_2\text{H}_3) = 5.0$ Hz, $^3J(\text{PH}) = 3.0$ Hz, $^3J(\text{H}_3\text{H}_5) = 2.0$ Hz, 1H, H₃), 3.32 (dddd, $^2J(\text{PH}) = 15.5$ Hz, $^2J(\text{HH}) = 13.8$ Hz, $^4J(\text{HH}) = 10.8$ Hz, $^4J(\text{HH}) = 8.0$ Hz, 1H, P⁺CH₂ (ring)),

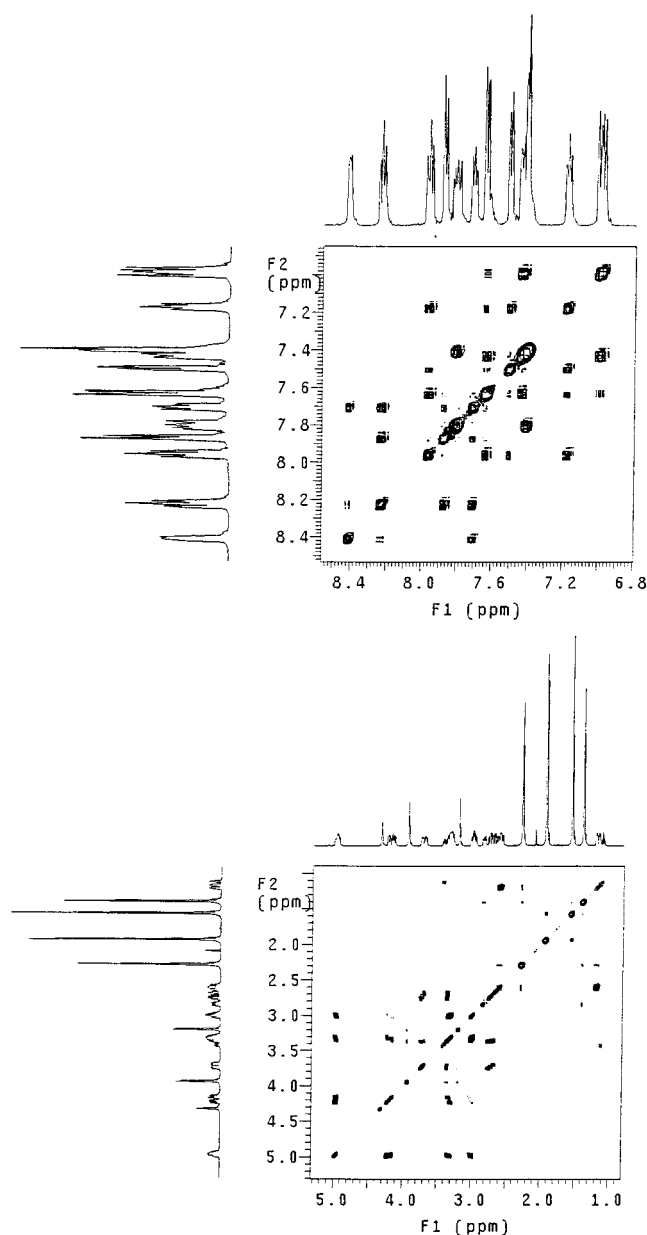


Figure 10. Expansions of the 499.8 MHz ^1H COSY-45 spectrum of **6a** in CD_3NO_2 in the aromatic (top) and aliphatic (bottom) regions.

3.21 (apparent q, $^2J(\text{PH}) = ^3J(\text{H}_1\text{H}_2) = ^4J(\text{H}_1\text{H}_5) = 1.5$ Hz, 1H, H_1), 3.00 (dddd, $^2J(\text{PH}) = 15.5$ Hz, $^2J(\text{HH}) = 13.8$ Hz, $^4J(\text{HH}) = 7.3$ Hz, $^4J(\text{HH}) = 1.5$ Hz, 1H, P^+CH_2 (ring)), 2.84 (dd, $^3J(\text{PH}) = 12.0$ Hz, $^2J(\text{PH}) = 7.5$ Hz, 1H, PdCH (ring)), 2.72 (dddd, $^3J(\text{PH}) = 36.0$ Hz, $^2J(\text{H}_3\text{H}_4) = 13.5$ Hz, $^3J(\text{H}_2\text{H}_4) = 10.5$ Hz, $^3J(\text{H}_4\text{H}_5) = 1.5$ Hz, 1H, H_4), 2.62 (dd, $^2J(\text{HH}) = 19.5$ Hz, $^3J(\text{PH}) = 13.0$ Hz, 1H, PyCH_2), 2.29 (q, $^5J(\text{HH}) = 0.5$ Hz, 3H, CH_3 (norbornene)), 1.94 (q, $^5J(\text{HH}) = 0.5$ Hz, 3H, CH_3 (P^+ ring)), 1.57 (q, $^5J(\text{HH}) = 0.5$ Hz, 3H, CH_3 (P^+ ring)), 1.40 (q, $^5J(\text{HH}) = 0.5$ Hz, 3H, CH_3 (norbornene)), 1.20 (d, $^2J(\text{HH}) = 19.5$ Hz, 1H, PyCH_2). $^{13}\text{C}\{^1\text{H}\}$ NMR (CD_3NO_2): δ 164.31 (C_6), 158.62 (d, $^3J(\text{PC}) = 5.0$ Hz, C_6), 151.41 (C_a), 151.26 (C_d), 141.56 (C_c), 140.31 (C_c), 136.56 (dd, $^2J(\text{PC}) = 8.8$ Hz, $^4J(\text{PC}) = 1.0$ Hz, C_6), 134.98 (C_5), 134.32 (C_5), 133.83 (d, $^4J(\text{PC}) = 2.9$ Hz, C_p), 133.26 (d, $^4J(\text{PC}) = 2.4$ Hz, C_p), 132.35 (d, $^2J(\text{PC}) = 9.4$ Hz, C_o), 129.70 (d, $^3J(\text{PC}) = 7.8$ Hz, C_m), 129.62 (d, $^2J(\text{PC}) = 5.3$ Hz, C_o), 129.58 (d, $^3J(\text{PC}) = 10.7$ Hz, C_m), 128.50 (C_d), 126.46 (d, $^6J(\text{PC}) = 1.0$ Hz, C_o), 126.27 (d, $^4J(\text{PC}) = 2.6$ Hz, C_d), 125.31 (d, $^1J(\text{PC}) = 75.3$ Hz, C_i), 125.15 (d, $^2J(\text{PC}) = 18.4$ Hz, C_o), 122.57 (d, $^1J(\text{PC}) = 73.0$ Hz, C_i), 50.16 (d, $^1J(\text{PC}) = 32.4$ Hz, C_1), 46.57 (d, $^2J(\text{PC}) = 17.5$ Hz, C_2), 45.72 (d, $^1J(\text{PC}) = 33.6$ Hz, C_4), 34.70 (d, $^2J(\text{PC}) = 51.0$ Hz, PyCH_2), 33.69 (d, $^2J(\text{PC}) = 27.9$ Hz, C_3), 32.85 (d, $^1J(\text{PC}) = 6.0$ Hz, P^+CH_2),

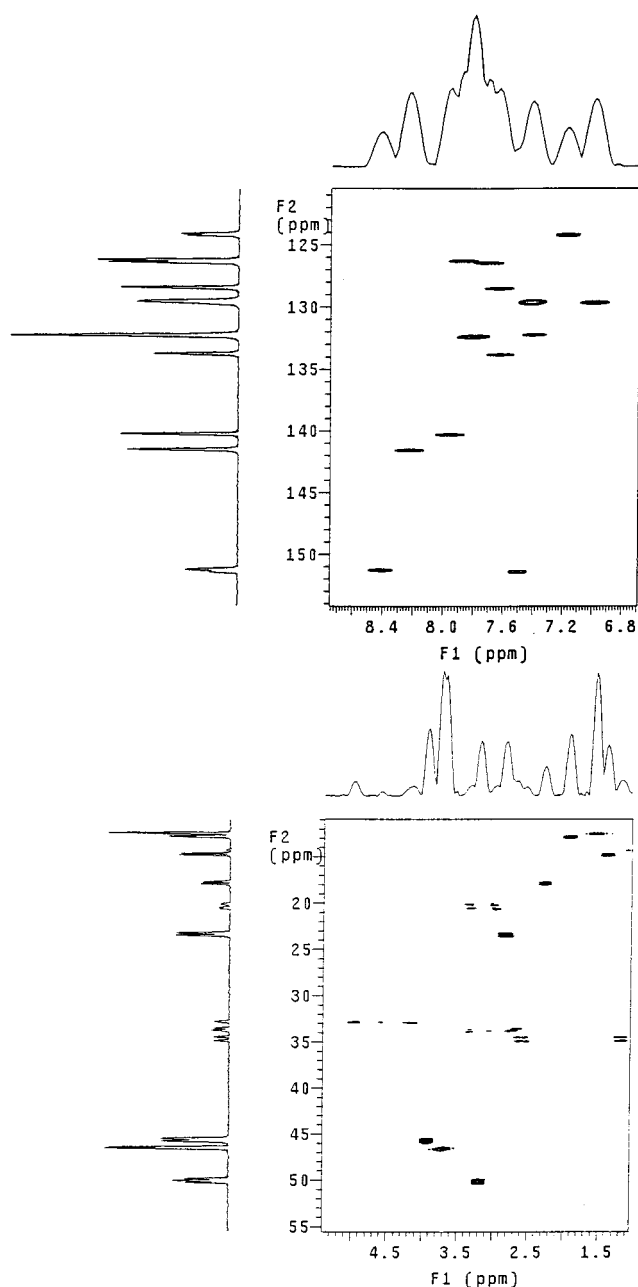


Figure 11. Expansions of the 125.7 MHz $^{13}\text{C}/^1\text{H}$ HETCOR spectrum of **6a** in CD_3NO_2 in the aromatic (top) and aliphatic (bottom) regions.

23.44 (d, $^1J(\text{PC}) = 32.8$ Hz, PdCH), 17.84 (d, $^3J(\text{PC}) = 16.0$ Hz, CH_3 (P^+ ring)), 14.75 (d, $^3J(\text{PC}) = 13.2$ Hz, CH_3 (norbornene)), 12.83 (d, $^3J(\text{PC}) = 3.4$ Hz, CH_3 (P^+ ring)), 12.49 (d, $^3J(\text{PC}) = 3.3$ Hz, CH_3 (norbornene)). Expansions of the COSY and $^{13}\text{C}/^1\text{H}$ HETCOR spectra that were essential for the assignments of the ^1H and ^{13}C chemical shifts are shown in Figures 10 and 11, respectively.

C. Kinetics Measurements. Solutions containing 100 mg of $[(\text{DMPP})_2\text{M}(\text{NO}_3)_2]$ and 2.2 equiv of the dienophile in 4 mL of CH_3CN and 1 mL of CD_3NO_2 were placed in 10 mm NMR tubes. The reactions were monitored by 202.3 MHz $^{31}\text{P}\{^1\text{H}\}$ NMR spectroscopy at 40 $^\circ\text{C}$ using the instruments temperature regulation (± 1 $^\circ\text{C}$) and kinetics routine. Typically, 200 transients were acquired for each time interval.

D. X-ray Data Collection and Processing. Crystals of the complexes were obtained from acetone/ether mixtures, mounted on glass fibers coated with epoxy, and placed on a Siemens P4 diffractometer. Intensity data were taken in the ω mode at 298 K with Mo K α graphite-monochromated radiation ($\lambda = 0.71073$ \AA). Three check reflections monitored every 100 reflections showed random ($< 2\%$) variation during

the data collections. The data were corrected for Lorentz and polarization effects and for absorption using an empirical model derived from azimuthal data collections, except for the case of **4b**, for which XABS2³⁸ was used. Scattering factors and corrections for anomalous dispersions were taken from a standard source.³⁹ Calculations were performed with the Siemens SHELXTL PLUS version 5.03 and 5.10 software packages on a personal computer. The structures were solved by direct (**1a**, **4a**, **5b**) or Patterson (**1b**, **2a**, **2b**, **3b**, **4b**, **6a**) methods. Anisotropic thermal

parameters were assigned to all non-hydrogen atoms, and hydrogen atoms were refined at calculated positions with a riding model in which the C–H vector was fixed at 0.96 Å.

Acknowledgment. This research was supported by an award from the Research Corp., for which we express our grateful appreciation.

Supporting Information Available: X-ray crystallographic files, in CIF format, for the structure determinations of **1a**, **1b**, **2a**, **2b**, **3b**, **4a**, **4b**, **5b**, and **6a**. This material is available free of charge via the Internet at <http://pubs.acs.org>.

IC990885J

(38) Parkins, S.; Moezzi, B.; Hope, H. XABS2: An empirical absorption corrections program. *J. Appl. Crystallogr.* **1995**, 53–56.

(39) *International Tables for X-ray Crystallography*; Reidel: Boston, MA, 1992; Vol. C.